

REVIEW OF QUASI-ELASTIC CHARGE-EXCHANGE DATA IN THE NUCLEON–DEUTERON BREAKUP REACTION

*F. Lehar*¹

Czech Technical University in Prague, IEAP, Prague, Czech Republic

*C. Wilkin*²

Physics and Astronomy Department, UCL, London, UK

The available data on the forward charge exchange of nucleons on the deuteron up to 2 GeV/nucleon are reviewed. The value of the inclusive $nd \rightarrow pnn/np \rightarrow pn$ cross section ratio is sensitive to the fraction of spin-independent neutron–proton backward scattering. The measurements of the polarisation transfer in $d(\vec{n}, \vec{p})\{nn\}$ or the deuteron analysing power in $p(\vec{d}, \{pp\})n$ in high-resolution experiments, where the final nn or pp pair emerge at low excitation energy, depend upon the longitudinal and transverse spin–spin np amplitudes. The relation between these types of experiments is discussed and the results compared with predictions of the impulse approximation model in order to see what new constraints they can bring to the neutron–proton database.

Описываются существующие данные по перезарядке нуклонов на дейтроне до энергии 2 ГэВ/нуклон. Значение отношения $nd \rightarrow pnn/np \rightarrow pn$ инклюзивного эффективного сечения чувствительно к нейтрон-протонному рассеянию назад, зависящему от спина. Измерения параметра передачи поляризации в реакции $d(\vec{n}, \vec{p})\{nn\}$ или анализирующей способности в экспериментах $p(\vec{d}, \{pp\})n$ с высоким разрешением, где конечная nn - или pp -пара вылетает с низкой энергией возбуждения, зависят от продольных или поперечных спин-спиновых np -амплитуд. Обсуждается связь между экспериментами такого типа. Результаты сравниваются с предсказаниями модели импульсного приближения для того, чтобы выявить новые ограничения, которые можно добавить к нейтрон-протонной базе данных.

PACS: 13.75.Cs; 25.40.Kv; 25.10.+s

1. INTRODUCTION

The charge exchange of neutrons or protons on the deuteron has a very long history. The first theoretical papers that dealt with the subject seem to date from the beginning of the 1950s with papers by Chew [1,2], Gluckstein and Bethe [3], and Pomeranchuk [4]. The first two groups were strongly influenced by the measurements of the differential cross section of

¹E-mail: lehar@mail.utef.cvut.cz

²E-mail: cw@hep.ucl.ac.uk

the $d(n, p)$ reaction that were then being undertaken at UCRL by Powell [5]. Apart from Coulomb effects, by charge symmetry the cross section for this reaction should be the same as that for $d(p, n)$. The spectrum of the emerging neutron in the forward direction here shows a very strong peaking for an energy that is only a little below that of the incident proton beam. There was therefore much interest in using the reaction as a means of producing a good quality neutron beam up to what was then «high» energies, i.e., a few hundred MeV. The theory of this proposal was further developed by Watson [6], Shmushkevich [7], Migdal [8], and Lapidus [9].

Since we have recently reviewed the phenomenology of the $d(n, p)$ and $d(p, n)$ charge exchange [10], the theory will not be treated here in any detail. The aim of the present paper is rather to discuss the database of the existing inclusive and exclusive measurements and make comparisons with the information that is available from neutron–proton elastic scattering data.

The proton and neutron bound in the deuterons are in a superposition of 3S_1 and 3D_1 states and their spins are parallel. On the other hand, if the four-momentum transfer $t = -q^2$ between the incident neutron and final proton in the $nd \rightarrow p\{nn\}$ reaction is very small, the Pauli principle demands that the two emerging neutrons be in the spin-singlet states 1S_0 and 1D_2 . In impulse (single-scattering) approximation, we would then expect the transition amplitude to be proportional to a spin-flip isospin-flip nucleon–nucleon scattering amplitude times a form factor that represents the overlap of the initial spin-triplet deuteron wave function with that of the unbound (scattering-state) nn wave function. The peaking observed in the energy spectrum of the outgoing proton is due to the huge neutron–neutron scattering length, which leads to a very strong final-state interaction (FSI) between the two neutrons.

A detailed evaluation of the proton spectrum from the $d(n, p)nn$ reaction would clearly depend upon the deuteron and nn wave functions, i.e., upon low-energy nuclear physics. However, a major advance was made by Dean [11, 12]. He showed that, if one integrated over all the proton energies, there was a closure sum rule where all the dependence on the nn wave function vanished:

$$\left(\frac{d\sigma}{dt}\right)_{nd \rightarrow p\{nn\}} = (1 - F(q)) \left(\frac{d\sigma}{dt}\right)_{np \rightarrow pn}^{\text{SI}} + \left[1 - \frac{1}{3}F(q)\right] \left(\frac{d\sigma}{dt}\right)_{np \rightarrow pn}^{\text{SF}}, \quad (1.1)$$

where $F(q)$ is the deuteron form factor. Here the neutron–proton differential cross section is split into two parts that represent the contribution that is independent of any spin transfer (SI) between the initial neutron and final proton and one where there is a spin flip (SF).

If the beam energy is high, then in the forward direction $q \approx 0$, $F(0) = 1$, and Eq.(1.1) reduces to

$$\left(\frac{d\sigma}{dt}\right)_{nd \rightarrow p\{nn\}} = \frac{2}{3} \left(\frac{d\sigma}{dt}\right)_{np \rightarrow pn}^{\text{SF}}. \quad (1.2)$$

There are modifications to Eq.(1.1) through the deuteron D state though these do not affect the forward limit of Eq.(1.2) [11–13]. As a consequence, the ratio

$$R_{np}(0) = \left(\frac{d\sigma}{dt}\right)_{nd \rightarrow p\{nn\}} / \left(\frac{d\sigma}{dt}\right)_{np \rightarrow pn} = \frac{2}{3} \left(\frac{d\sigma}{dt}\right)_{np \rightarrow pn}^{\text{SF}} / \left(\frac{d\sigma}{dt}\right)_{np \rightarrow pn} \quad (1.3)$$

is equal to two thirds of the fraction of spin flip in $np \rightarrow pn$ between the incident neutron and proton outgoing in the beam direction. It is because the ratio of two unpolarised cross

sections can give information about the spin dependence of neutron–proton scattering that so many groups have made experimental studies in the field and these are discussed in Sec. 3. Of course, for this to be a useful interpretation of the cross section ratio the energy has to be sufficiently high for the Dean sum rule to converge before any phase space limitations become important. The longitudinal momentum transfer must be negligible and terms other than the $np \rightarrow pn$ impulse approximation should not contribute significantly to the evaluation of the sum rule. Although the strong NN FSI helps with these concerns, all the caveats indicate that Eq. (1.3) would provide at best only a qualitative description of data at the lower energies.

The alternative approach is not to use a sum rule but rather to measure the excitation energy in the outgoing dineutron or diproton with good resolution and then evaluate the impulse approximation directly by using deuteron and NN scattering wave functions, i.e., input information from low-energy nuclear physics. This avoids the questions of the convergence of the sum rule and so might yield useful results down to lower energies. A second important feature of the $d(p, n)pp$ reaction in these conditions is that the polarisation transfer between the initial proton and the final neutron is expected to be very large, provided that the excitation energy E_{pp} in the final two-proton system is constrained to be only a few MeV [14,15]. In fact the reaction has been used by several groups to furnish a polarised neutron beam [16–18] but also as a means to study neutron–proton charge-exchange observables, as described in Sec. 4.

Bugg and Wilkin [13,19] realised that in the small E_{pp} limit the deuteron tensor analysing powers in the $p(\vec{d}, \{pp\})n$ reaction should also be large and with a significant angular structure that was sensitive to the differences between the neutron–proton spin-flip amplitudes. This realisation provided an impetus for the study of high-resolution $p(\vec{d}, \{pp\})n$ experiments that are detailed in Sec. 5.

The inclusive (p, n) or (n, p) measurements of Sec. 3 and the high-resolution ones of Secs. 4 and 5 are in fact sensitive to exactly the same physics input. To make this explicit, we outline in Sec. 2 the necessary np formalism through which one can relate the forward values of R_{np} or R_{pn} , the polarisation transfer in $d(\vec{n}, \vec{p})nn$ and the deuteron tensor analysing power in $p(\vec{d}, \{pp\})n$ in impulse approximation to the longitudinal and transverse polarisation transfer coefficients in neutron–proton elastic scattering. Predictions for the observables are made there using an up-to-date phase shift analysis.

Data are available on the R_{np} and R_{pn} parameters in, respectively, inclusive $d(n, p)nn$ and $d(p, n)pp$ reactions at energies that range from tens of MeV up to 2 GeV and the features of the individual experiments are examined in Sec. 3, where the results are compared to the predictions of the phase shift analysis.

Polarisation transfer data have become steadily more reliable with time, with firmer control over the NN excitation energies and better calibrated polarisation measurements so that the data described in Sec. 3 now extend from 10 up to 800 MeV.

Four experimental programmes were devoted to the study of the cross section and tensor analysing powers of the $p(\vec{d}, \{pp\})n$ reaction using very different experimental techniques. Their procedures are described in Sec. 5 and the results compared with the predictions of the plane-wave impulse approximation. In general this gives a reasonable description of the data out to a three-momentum transfer of $q \approx m_\pi$ by which point multiple scatterings might become important. These data are however only available in an energy domain where the neutron–proton database is extensive and reliable and the possible extensions are also outlined there.

The comparison between the sum-rule and high-resolution approaches is one of the subjects that is addressed in our conclusions of Sec. 6. The consistency between the information obtained from the $d(\vec{n}, \vec{p})nn$ and $p(\vec{d}, \{pp\})n$ reactions in the forward direction is striking, and the belief is expressed that this must contribute positively to our knowledge of the neutron–proton charge-exchange phenomenology.

2. NEUTRON–PROTON AND NUCLEON–DEUTERON OBSERVABLES

We have shown that the input necessary for the evaluation of the forward charge-exchange observables can be expressed as combinations of *pure* linearly independent $np \rightarrow np$ observables evaluated in the backward direction [10]. Although the expressions are independent of the scattering amplitude representation, for our purposes it is simplest to use the results of polarisation transfer experiments. The NN formalism gives two series of polarisation transfer parameters that are mutually dependent [20]. Using the notation X_{srbt} for experiments with measured spin orientations for the scattered (s), recoil (r), beam (b), and target (t) particles, we have either the polarisation transfer from the beam to recoil particles,

$$\frac{d\sigma}{dt} K_{0rb0} = \frac{1}{4} \text{Tr} \{ \sigma_{2r} M \sigma_{1b} M^\dagger \}, \quad (2.1)$$

or the polarisation transfer from the target to the scattered particle

$$\frac{d\sigma}{dt} K_{s00t} = \frac{1}{4} \text{Tr} \{ \sigma_{1s} M \sigma_{2t} M^\dagger \}. \quad (2.2)$$

Here σ_{1s} , σ_{1b} , σ_{2t} , and σ_{2r} are the corresponding Pauli matrices and M is the scattering matrix. The unpolarised invariant elastic scattering cross section

$$\frac{d\sigma}{dt} = \frac{\pi}{k^2} \frac{d\sigma}{d\Omega} = \frac{1}{4} \text{Tr} \{ M M^\dagger \}, \quad (2.3)$$

where k is the momentum in the CM frame and t is the four-momentum transfer.

A first series of parameters describes the scattering of a polarised neutron beam on an unpolarised proton target, where the polarisation of the final outgoing protons is measured by an analyser through a second scattering. The spins of the incident neutrons can be oriented either perpendicularly or longitudinally with respect to the beam direction, with the final proton polarisations being measured in the same directions. At $\theta_{\text{CM}} = \pi$ there are two independent parameters, $K_{0nn0}(\pi)$ and $K_{0ll0}(\pi)$, referring respectively to the transverse (n) and longitudinal (l) directions. It was shown in [10] that the forward $d(n, p)n/p(n, p)n$ cross section ratio can be written in terms of these as

$$R_{np}(0) = \frac{1}{6} \{ 3 - 2K_{0nn0}(\pi) - K_{0ll0}(\pi) \}. \quad (2.4)$$

A second series of parameters describes the scattering of an unpolarised neutron beam on a polarised proton target, where it is the polarisation of the final outgoing neutron that is determined. This leads to the alternative expression for $R_{np}(0)$:

$$R_{np}(0) = \frac{1}{6} \{ 3 - 2K_{n00n}(\pi) + K_{l00l}(\pi) \}, \quad (2.5)$$

where $K_{n00n}(\pi) = K_{0nn0}(\pi)$ but $K_{l00l}(\pi) = -K_{0ll0}(\pi)$. Other equivalent relations are to be found in [20].

It cannot be stressed enough that the small-angle (n, p) charge exchange on the deuteron is sensitive to the spin transfer from the incident neutron to the outgoing proton and NOT that to the outgoing neutron. The latter observables are called the depolarisation parameters D which, for example, are given in the case of a polarised target by

$$\frac{d\sigma}{dt} D_{0r0t} = \frac{1}{4} \text{Tr} \{ \sigma_{2r} M \sigma_{1t} M^\dagger \}. \quad (2.6)$$

If one were to evaluate instead of Eq. (2.5) the combination

$$r_{np}(0) = \frac{1}{6} \{ 3 - 2D_{0n0n}(\pi) - D_{0l0l}(\pi) \}, \quad (2.7)$$

then one would get a completely independent (and wrong) answer. Using the SAID SP07 phase shift solution at 100 MeV, one finds that $R_{np}(0) = 0.60$, while $r_{np}(0) = 0.13$. Hence one has to be very careful with the statement that the $np \rightarrow np$ spin dependence in the backward direction is weak or strong. It depends entirely on which particles one is discussing.

In plane-wave impulse approximation, the one non-vanishing deuteron tensor analysing power in the $p(d, \{pp\})n$ reaction in the forward direction can be expressed in terms of the same spin-transfer parameters, provided that the excitation energy in the pp system is very small such that it is in the 1S_0 state [10, 13]:

$$A_{NN}(0) = \frac{2(K_{0ll0}(\pi) - K_{0nn0}(\pi))}{3 - K_{0ll0}(\pi) - 2K_{0nn0}(\pi)}. \quad (2.8)$$

In an attempt to minimise confusion, observables in the nucleon–deuteron sector will be labelled with capital letters and only carry two subscripts.

In the same approximation, the longitudinal and transverse spin-transfer parameters in $d(\vec{p}, \vec{n})pp$ between the initial proton and the final neutron emerging in the beam direction are similarly given by

$$K_{LL}(0) = - \left[\frac{1 - 3K_{0ll0}(\pi) + 2K_{0nn0}(\pi)}{3 - K_{0ll0}(\pi) - 2K_{0nn0}(\pi)} \right], \quad (2.9)$$

$$K_{NN}(0) = - \left[\frac{1 + K_{0ll0}(\pi) - 2K_{0nn0}(\pi)}{3 - K_{0ll0}(\pi) - 2K_{0nn0}(\pi)} \right].$$

Independent of any theoretical model, these parameters are related by [14, 21]

$$K_{LL}(0) + 2K_{NN}(0) = -1. \quad (2.10)$$

Equally generally, in the 1S_0 limit the forward longitudinal and transverse deuteron tensor analysing powers are trivially related;

$$A_{LL}(0) = -2A_{NN}(0), \quad (2.11)$$

and these are in turn connected to the spin-transfer coefficients through [21]

$$A_{LL}(0) = -\frac{1 + 3K_{LL}(0)}{2} \quad \text{or} \quad A_{NN}(0) = -\frac{1 + 3K_{NN}(0)}{2}. \quad (2.12)$$

Table 1. Values of the np backward differential cross section in the CM system $d\sigma/d\Omega$, and in invariant normalisation $d\sigma/dt$. Also shown are the forward $d(n,p)n/p(n,p)n$ ratio $R_{np}(0)$, the longitudinal polarisation transfer parameter $K_{LL}(0)$ in the $d(\vec{p}, \vec{n})pp$ reaction, and the deuteron analysing power $A_{NN}(0)$ in the $p(\vec{d}, \{pp\})n$ reaction at the same energy per nucleon. These have all been evaluated from the plane wave impulse approximation using the energy-dependent PSA of Arndt et al., solution SP07 [22]

T_n , GeV	$d\sigma/d\Omega$, mb/sr	$d\sigma/dt$, mb/(GeV/c) ²	$R_{np}(0)$	$K_{LL}(0)$	$A_{NN}(0)$
0.010	78.74	52728	0.404	-0.370	-0.027
0.020	42.92	14371	0.433	-0.273	0.045
0.030	29.84	6661	0.466	-0.167	0.125
0.040	23.56	3944	0.498	-0.085	0.186
0.050	20.11	2693	0.525	-0.030	0.227
0.060	18.04	2013	0.547	0.000	0.250
0.070	16.71	1599	0.565	0.014	0.260
0.080	15.81	1323	0.579	0.014	0.261
0.090	15.17	1129	0.591	0.006	0.255
0.100	14.68	983	0.600	-0.008	0.244
0.120	13.98	780	0.613	-0.048	0.214
0.150	13.27	592	0.627	-0.118	0.162
0.200	12.46	417	0.639	-0.231	0.077
0.250	11.88	318	0.645	-0.327	0.005
0.300	11.45	255	0.645	-0.405	-0.054
0.350	11.19	214	0.644	-0.472	-0.104
0.400	11.02	184	0.639	-0.530	-0.148
0.450	10.88	162	0.631	-0.582	-0.186
0.500	10.62	142	0.621	-0.630	-0.223
0.550	10.10	123	0.608	-0.678	-0.259
0.600	9.45	105	0.596	-0.726	-0.295
0.650	9.07	93.4	0.588	-0.762	-0.321
0.700	8.96	85.8	0.586	-0.773	-0.330
0.750	8.95	79.9	0.588	-0.769	-0.327
0.800	8.93	74.7	0.592	-0.761	-0.321
0.850	8.98	69.9	0.596	-0.754	-0.315
0.900	8.81	65.5	0.601	-0.748	-0.311
0.950	8.73	61.5	0.605	-0.744	-0.308
1.000	8.65	57.9	0.609	-0.740	-0.305
1.050	8.57	54.7	0.613	-0.737	-0.303
1.100	8.50	51.7	0.616	-0.735	-0.302
1.150	8.44	49.1	0.620	-0.735	-0.301
1.200	8.40	46.8	0.623	-0.736	-0.302
1.250	8.38	44.9	0.626	-0.739	-0.304
1.300	8.39	43.2	0.629	-0.740	-0.308

We stress once again that, although Eqs. (2.8) and (2.9) are model-dependent, Eqs. (2.10), (2.11), and (2.12) are exact if the final pp system is in the 1S_0 state.

The variation of the np backward elastic cross section with energy and the values of $R_{np}(0)$, $A_{NN}(0)$, and $K_{LL}(0)$ have been calculated using the energy-dependent GW/VPI

PSA solution SP07 [22] and are listed in Table 1. The relations between the observables used in [22] and [20] are to be found in the SAID program.

The GW/VPI PSA for proton–proton scattering can be used up to 3.0 GeV but, according to the authors, the predictions are at best qualitative above 2.5 GeV [22]. Because this is an energy-dependent analysis, one cannot use the SAID program to estimate the errors of any observable. Although the equivalent PSA for neutron–proton scattering was carried out up to 1.3 GeV, very few spin-dependent observables have been measured above 1.1 GeV.

Let us summarise the present status of the np database at intermediate energies. About 2000 spin-dependent np elastic scattering data points, involving 11 to 13 independent observables, were determined at SATURNE 2 over large angular intervals mainly between 0.8 and 1.1 GeV [23,24]. A comparable amount of np data in the region from 0.5 to 0.8 GeV was measured at LAMPF [25] and in the energy interval from 0.2 to 0.56 GeV at PSI [26]. The TRIUMF group also contributed significantly up to 0.515 GeV [27].

The SATURNE 2 and the PSI data were together sufficient, not only to implement the PSA procedure, but also to perform a direct amplitude reconstruction at several energies and angles. It appears that the spin-dependent data are more or less sufficient for this procedure at the lower energies, whereas above 0.8 GeV there is a lack of np differential cross section data, mainly at intermediate angles.

3. MEASUREMENTS OF UNPOLARISED QUASI-ELASTIC CHARGE-EXCHANGE OBSERVABLES

3.1. The (n, p) Experiments. The first measurement of the $d(n, p)$ differential cross section was undertaken at UCRL by Powell in 1951 [5]. These data at 90 MeV were reported by Chew [2], though only in graphical form, and from this one deduces that $R_{np}(0) = 0.40 \pm 0.04$. A year later Cladis, Hadley, and Hess, working also at the UCRL synchrocyclotron, published data obtained with the 270 MeV neutron beam [28]. Their value of 0.71 ± 0.02 for the ratio of their own deuteron/hydrogen data is clearly above the permitted limit of $2/3$ by more than the claimed error bar. This may be connected with the very broad energy spectrum of the incident neutron beam, which had a FWHM ≈ 100 MeV.

At the Dubna synchrocyclotron the first measurements were carried out by Dzhelepov et al. [29, 30] in 1952–1954 with a 380 MeV neutron beam. Somewhat surprisingly, the authors considered their result, $R_{np}(0) = 0.20 \pm 0.04$, to be compatible with the UCRL measurements [5,28]. In fact, later more refined experiments [31] showed that the Dzhelepov et al. value was far too low and it should be discarded from the database.

At the end of that decade Larsen measured the same quantity at LRL Berkeley at a relatively high energy of 710 MeV and obtained $R_{np}(0) = 0.48 \pm 0.08$ [32]. However, no previous results were mentioned in his publication.

In his contribution to the 1962 CERN conference [33], Dzhelepov presented the angular dependence of $R_{np}(\theta)$ at 200 MeV. Although he noted that the authors of the experiment were Yu. Kazarinov, V. Kiselev, and Yu. Simonov, no reference was given and we have found no publication. Reading the value from a graph, one obtains $R_{np}(0) = 0.55 \pm 0.03$.

One advantage of working at very low energies, as was done in Moscow [34], is that one can obtain a neutron beam from the ${}^3\text{H}(d, n){}^4\text{He}$ reaction that is almost monochromatic. At 13.9 MeV there is clearly no hope at all of fulfilling the conditions of the Dean sum rule

Table 2. The $R_{np}(0)$ data measured using the $d(n,p)nn$ reaction. The total estimated uncertainties quoted do not take into account the influence of the different possible choices on the cut on the final proton momentum

T_n , MeV	$R_{np}(0)$	Facility	Year	Ref.
13.9	0.19	Moscow	1965	[34]
90.0	0.40 ± 0.04	UCRL	1951	[5]
152.0	0.65 ± 0.10	Harvard	1966	[36]
200.0	0.55 ± 0.03	JINR DLNP	1962	[33]
270.0	0.71 ± 0.02	UCRL	1952	[28]
299.7	0.65 ± 0.03	PSI	1988	[31]
319.8	0.64 ± 0.03	PSI	1988	[31]
339.7	0.64 ± 0.03	PSI	1988	[31]
359.6	0.63 ± 0.03	PSI	1988	[31]
379.6	0.64 ± 0.03	PSI	1988	[31]
380.0	0.20 ± 0.04	INP Dubna	1955	[29]
399.7	0.61 ± 0.03	PSI	1988	[31]
419.8	0.62 ± 0.03	PSI	1988	[31]
440.0	0.63 ± 0.03	PSI	1988	[31]
460.1	0.61 ± 0.03	PSI	1988	[31]
480.4	0.61 ± 0.03	PSI	1988	[31]
500.9	0.59 ± 0.03	PSI	1988	[31]
521.1	0.60 ± 0.03	PSI	1988	[31]
539.4	0.62 ± 0.03	PSI	1988	[31]
550.0	0.59 ± 0.05	JINR VBLHEP	2009	[41]
557.4	0.63 ± 0.03	PSI	1988	[31]
710.0	0.48 ± 0.08	LRL	1960	[32]
794.0	0.56 ± 0.04	LAMPF	1978	[37]
800.0	0.55 ± 0.02	JINR VBLHEP	2009	[41]
1000	0.55 ± 0.03	JINR VBLHEP	2009	[41]
1200	0.55 ± 0.02	JINR VBLHEP	2009	[41]
1400	0.58 ± 0.04	JINR VBLHEP	2009	[41]
1800	0.57 ± 0.03	JINR VBLHEP	2009	[41]
2000	0.56 ± 0.05	JINR VBLHEP	2009	[41]

so that the value given in Table 2 was obtained with a very severe cut. Instead, the group concentrated on the final-state interaction region of the two neutrons which, in some ways, is similar to the approach of the high-resolution experiments to be discussed in Sec. 5. By comparing the data with the $d(p,n)pp$ results of [35], it was possible to see the effects of the Coulomb repulsion when the two protons were detected in the FSI peak.

Though the value obtained by Measday [36] at 152 MeV has quite a large error bar, $R_{np}(0) = 0.65 \pm 0.10$, this seems to be mainly an overall systematic effect because the variation of the result with angle is very smooth. These results show how $R_{np}(\theta)$ approaches two thirds as the momentum transfer gets large and the Pauli blocking becomes less important.

The 794 MeV measurement from LAMPF [37] is especially detailed, with very fine steps in momentum transfer. Extrapolated to $t = 0$, it yields $R_{np}(0) = 0.56 \pm 0.04$. However, the

authors suggest that the true value might be a little higher than this due to the cut that they imposed upon the lowest proton momentum considered.

By far the most extensive $d(n, p)nn$ data set at medium energies was obtained by the Freiburg group working at PSI, the results of which are only available in the form of a diploma thesis [31]. However, the setup used by the group for neutron–proton backward elastic scattering is described in [38]. The PSI neutron beam was produced through the interaction of an intense 589 MeV proton beam with a thick nuclear target. This delivered pulses with widths of less than 1 ns and bunch spacings of 20 or 60 ns. Combining this with a time-of-flight path of 61 m allowed for a good selection of the neutron momentum, with an average resolution of about 3% FWHM. Data were reported at fourteen neutron energies from 300 to 560 MeV, i.e., above the threshold for pion production so that the results could be normalised using the cross section for $np \rightarrow d\pi^0$, which was measured in parallel [38]. Over this range $R_{np}(0)$ showed very little energy dependence, with an average value of 0.62 ± 0.01 , which is quite close to the upper limit of $2/3$.

At the JINR VBLHE, Dubna, a high quality quasi-monoenergetic polarised neutron beam was extracted in 1994 from the Synchrophasotron for the purposes of the $\Delta\sigma_L(np)$ measurements [39, 40], though this accelerator was stopped in 2005. Polarised deuterons are not yet available from the JINR Nuclotron but, on the other hand, intense unpolarised beams with very long spills could be obtained from this machine. Since the final $\Delta\sigma_L$ set-up included a spectrometer, the study of the energy dependence of $R_{np}(0)$ could be extended up to 2.0 GeV through the measurement of seven points [41]. That at 550 MeV agrees very well with the neighbouring PSI point [31], while the one at 800 MeV is consistent with the LAMPF measurement [37]. Since the values of $R_{np}(0)$ above 1 GeV could not have been reliably predicted from previous data, the Nuclotron measurements in the interval $1.0 < T_n < 2$ GeV can be considered to be an important achievement in this field. It would be worthwhile to complete these experiments by measurements in smaller energy steps in order to recognise possible anomalies or structures. It is also desirable to extend the investigated interval up to the highest neutron energy at the Nuclotron (≈ 3.7 GeV) since such measurements are currently only possible at this accelerator.

The data on $R_{np}(0)$ from the $d(n, p)nn$ experiments discussed above are summarised in Table 2, where the kinetic energy, facility, year of publication, and reference are also listed. Several original papers show the values of the angular distribution of the charge-exchange cross section on the deuteron. In such cases, the $R_{np}(0)$ listed here were obtained using the predictions for the free forward np charge-exchange cross sections taken from the SAID program (solution SP07) [22]. These values are shown in Table 1.

3.2. The (p, n) Experiments. Although high-quality proton beams have been available at many facilities, the evaluation of a $R_{pn}(0)$ ratio from $d(p, n)pp$ experiments requires the division of this cross section by that for the charge exchange on a nucleon target. Where necessary, we have done this using the predictions of the SP07 SAID solution [22] given in Table 1. Given also the difficulties in obtaining absolute normalisations when detecting neutrons, we consider that in general the results obtained using neutron beams are likely to be more reliable.

The low-energy data of Wong et al. [35] at 13.5 MeV do show evidence of a peak for the highest momentum neutrons but this is sitting on a background coming from other breakup mechanisms that are probably not associated with charge exchange. The value given in Table 3 without an error bar is therefore purely indicative.

Table 3. The $R_{pn}(0)$ data measured using the $d(p,n)pp$ reaction. The total estimated uncertainties quoted do not take into account the influence of the different possible choices on the cut on the final neutron momentum

$T_{\text{kin}}, \text{MeV}$	$R_{pn}(0)$	Facility	Year	Ref.
13.5	0.18	Livermore	1959	[35]
30.1	0.14 ± 0.04	RHEL	1967	[43]
50.0	0.24 ± 0.06	RHEL	1967	[43]
95.0	0.48 ± 0.03	Harvard	1953	[42]
94.7	0.59 ± 0.03	Harwell	1967	[44]
135.0	0.65 ± 0.15	Harwell	1965	[46]
143.9	0.60 ± 0.06	Harwell	1967	[44]
647.0	0.60 ± 0.08	LAMPF	1976	[45]
800.0	0.66 ± 0.08	LAMPF	1976	[45]

In 1953 Hofmann and Strauch [42], working at the Harvard University accelerator, published results on the interaction of 95 MeV protons with several nuclei and measured the $d(p,n)$ reaction for the first time. An estimation of the charge-exchange ratio from the plotted data gives $R_{pn}(0) = 0.48 \pm 0.03$.

The measurements at 30 and 50 MeV were made using the time-of-flight facility of the Rutherford Laboratory (RHEL) Proton Linear Accelerator [43]. The neutron spectrum, especially at 30 MeV, does not show a clear separation of the charge-exchange impulse contribution from other mechanisms and the Dean sum rule is far from being saturated. The same facility was used at higher energies of 95 and 144 MeV, where the target was once again deuterated polythene [44]. This allowed the spectrum to be studied up to a proton-proton excitation energy $E_{pp} \approx 14$ MeV when neutrons from reactions on the carbon in the target contributed. It was claimed that the cross sections obtained had an overall normalisation uncertainty of about $\pm 10\%$ and that the impulse approximation could describe the data within this error bar.

The highest energy (p,n) data were produced at LAMPF [45], where the charge-exchange peak was clearly separated from other mechanisms, including pion production, and the conditions for the use of the Dean sum rule were well satisfied. Their high value of $R_{pn}(0) = 0.66 \pm 0.08$ at 800 MeV would be reduced to 0.61 if the np data of Table 1 were used for normalisation instead of those available in 1976.

The approach by the UCL group working at $T_p = 135$ MeV at Harwell was utterly different to the others. They used a high-pressure Wilson cloud chamber triggered by counters, which resulted in a large fraction of 1740 photographs containing events [46]. This led to 1048 events of proton-deuteron collisions that were included in the final data analysis. Instead of detecting the neutron from the $d(p,n)pp$ reaction, the group measured both protons. In a sense therefore the experiment is similar to that of the Dubna bubble chamber group [47], but in inverted kinematics. Due to the geometry of the counter selection system, the apparatus was blind to protons that were emitted in a cone of laboratory angles $\theta_{\text{lab}} < 10^\circ$ with energies above 6 MeV. Although the corrections for the associate losses are model-dependent, these should not affect the neutrons emerging at small angles and the results were integrated down to a neutron kinetic energy that was 8 MeV below the maximum allowed. The differential cross

sections were compared to the plane-wave impulse approximation calculations of Castillejo and Singh [48].

The results from the various $d(p, n)pp$ experiments are summarised in Table 3.

3.3. The Unpolarised $dp \rightarrow ppn$ Reaction. In principle, far more information is available if the two final protons are measured in the deuteron charge-exchange reaction and not merely the outgoing neutron. This has been achieved by using a beam of deuterons with momentum $3.35 \text{ GeV}/c$ incident on the Dubna hydrogen bubble chamber. Because of the richness of the data contained, the experiment has had a very long history with several reanalyses [47, 49–52].

Of the seventeen different final channels studied, the largest number of events (over 10^5) was associated with deuteron breakup. These could be converted very reliably into cross sections by comparing the sum over all channels with the known total cross section. Corrections were made for the loss of elastic dp scattering events at very small angles. The $dp \rightarrow ppn$ events were divided into two categories, depending upon whether it was the neutron or one of the two protons that had the lowest momentum in the deuteron rest frame. This identification of the charge-retention or charge-exchange channels is expected to be subject to little ambiguity for small momentum transfers. With this definition, the total cross section for deuteron charge exchange was found to be $(5.85 \pm 0.05) \text{ mb}$.

The big advantage of the bubble chamber approach is that one can check many of the assumptions that are made in the analysis. The crucial one is, of course, the separation into the charge-exchange and charge-retention events. In the latter case the distribution of «spectator» momenta p_{sp} falls smoothly with p_{sp} , but in the charge-exchange sample there is a surplus of events for $p_{\text{sp}} \gtrsim 200 \text{ MeV}/c$ that may be associated with the virtual production of a $\Delta(1232)$ that de-excites through $\Delta N \rightarrow pp$. Perhaps a fifth of the charge-exchange cross section could be due to this mechanism [51], but, fortunately, such events necessarily involve significant momentum transfers and would not influence the extrapolation to $q = 0$.

After making corrections for events that have larger opening angles [47], the data analysis gives a value of

$$\left. \frac{d\sigma}{dt}(dp \rightarrow \{pp\}n) \right|_{t=0} = \frac{2}{3} \left. \frac{d\sigma^{\text{SF}}}{dt}(dp \rightarrow \{pp\}n) \right|_{t=0} = (30 \pm 4) \text{ mb}/(\text{GeV}/c)^2, \quad (3.1)$$

where σ^{SF} is the cross section corresponding to the spin flip from the initial proton to the final neutron and the $2/3$ factor comes from the Dean sum rule. Some of the above error arises from the estimation of the effects of the wide angle proton pairs and in the earlier publication of the group [52], where the same data set was treated somewhat differently, a lower value of $(25 \pm 3) \text{ mb}/(\text{GeV}/c)^2$ was obtained.

The Dubna bubble chamber measurement can lead to a relatively precise value of the average of the spin–spin amplitudes squared. Using Eq.(3.1), one obtains very similar information to that achieved with the high-resolution $dp \rightarrow \{pp\}n$ measurements to be discussed in Sec. 5 and with very competitive error bars. On the other hand, if the primary aim is to derive estimates for the spin-independent contribution to the forward np charge-exchange cross section, then it loses some of the simplicity and directness of the $d(n, p)nn/p(n, p)n$ comparison. This is because one has to evaluate the ratio of two independently measured numbers, each of which has its own normalisation uncertainty. The problem is compounded by the fact that, as we have seen from the direct (n, p) measurements of $R_{np}(0)$, the contribution of the spin-independent amplitude represents only a small fraction of the total.

Table 4. Summary of the available experimental data on the $R_{np}(0)$ ratio measured with the Dubna bubble chamber using the $dp \rightarrow \{pp\}n$ reaction. The kinetic energy quoted here is the energy per nucleon. The error bars reflect both the statistical and systematic uncertainties. Although the data sets are basically identical, the 2008 analysis [47] is believed to be the most reliable

T_{kin} , MeV	$R_{np}(0)$	Facility	Year	Ref.
977	0.43 ± 0.22	JINR VBLHE	1975	[49]
977	0.63 ± 0.12	JINR VBLHE	2002	[52]
977	0.55 ± 0.08	JINR VBLHEP	2008	[47]

In the earlier publications by the Dubna group, the necessary normalisation denominator was taken from the elastic neutron–proton scattering measurements of Shepard et al. at the Pennsylvania Proton Accelerator [53]. These were made at sixteen energies and over wide angular ranges. However, they disagreed strongly with all other existing np data, not only in the absolute values, but also in the shapes of angular distributions. This problem was already apparent at low energies, starting at 182 MeV. As a result, these data have long been discarded by physicists working in the field and they have been removed from phase shift analysis databases, e.g. from the Saclay–Geneva PSA in 1978 [54].

A much more reliable $np \rightarrow pn$ data set was provided by the ER54 group of Bizard et al. [55], numerical values of which are to be found in [56,57]. Fitting these data with two exponentials gives a forward cross section of $d\sigma/dt|_{t=0} = (54.7 \pm 0.2) \text{ mb}/(\text{GeV}/c)^2$, which the Dubna group used in their final publication [47]. It is very different from the Shepard et al. result [53] of $(36.5 \pm 1.4) \text{ mb}/(\text{GeV}/c)^2$, which the group quoted in their earlier work [52]. This difference, together with the changed analysis corrections, accounts for the diverse values of $R_{np}(0)$ from the same experiment that are given in Table 4.

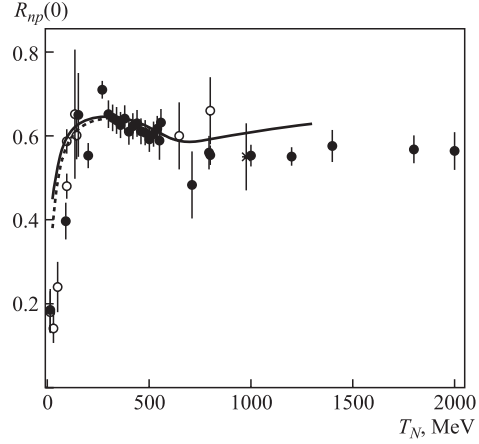
3.4. Data Summary. The values of $R_{np}(0)$ and $R_{pn}(0)$ from Tables 2 and 3 are shown in graphical form in Fig. 1, with only the early Dubna point [29] being omitted. The $p(d, 2p)$ values in Table 4 represent the results of increased statistics and a different analysis and only the point from the last publication is shown [47].

The first comparison of such data with np phase shift predictions was made in 1991 in a thesis from the Freiburg group [58], where both the GW/VPI [59] and Saclay–Geneva [54] were studied. The strong disagreement with the results of the PSI measurements [31] was due to the author misinterpreting the relevant quantity as being $r_{np}(0)$ of Eq. (2.7) instead of $R_{np}(0)$ of Eq. (2.4).

The correct predictions from the current GW/VPI phase shift analysis obtained on the basis of Eq. (2.4) are shown in Fig. 1 up to the limit of their validity at 1.3 GeV. The small values of $R_{np}(0)$ at low energies is in part due to the much greater importance of the spin-independent contribution there, as indicated by the phase shift predictions. There are effects arising also from the limited phase space but, when they are included (dashed curve), they change the results only marginally. A much greater influence is the cut that authors have to put onto the emerging neutron or proton to try to isolate the charge-exchange contribution from that of other mechanisms. This procedure becomes far more ambiguous at low energies when relatively severe cuts have to be imposed.

The data in Fig. 1 seem to be largest at around the lowest PSI point [31], where they get close to the allowed limit of 0.67. In fact, if the Glauber shadowing effect is taken into

Fig. 1. Experimental data on the $R_{np}(0)$ ratio taken in the forward direction. The closed circles are from the (n, p) data of Table 2, the open circles from the (p, n) data of Table 3, and the cross from the $(d, 2p)$ datum of Table 4. These results are compared to the predictions of Eq. (2.4) using the current SAID solution [22], which is available up to a laboratory kinetic energy of 1.3 GeV. The dashed curve takes into account the limited phase space available at the lower energies



account [60], this limit might be reduced to perhaps 0.63. As already shown by the phase shift analysis, the contribution from the spin-independent term is very small in this region. On the other hand, in the region from 1.0 to 1.3 GeV the phase shift curve lies systematically above the experimental data. Since the conditions for the Dean sum rule seem to be best satisfied at high energies, this suggests that the SAID solution underestimates the spin-independent contribution above 1 GeV. It has to be noted that the experimental np database is far less rich in this region.

4. POLARISATION TRANSFER MEASUREMENTS IN $d(\vec{p}, \vec{n})pp$

It was first suggested by Phillips [14] that the polarisation transfer in the charge-exchange reaction $d(\vec{p}, \vec{n})pp$ should be large provided that the excitation energy E_{pp} in the final pp system is small. Under such conditions the diproton is in the 1S_0 state so that there is a spin-flip transition from a $J^P = 1^+$ to a 0^+ configuration of the two nucleons. This spin-selection argument is only valid for the highest neutron momentum since, as E_{pp} increases, P and higher waves enter and the polarisation signal reduces [15]. Nevertheless, the reaction has been used successfully by several groups to produce polarised neutron beams [16–18].

In the 1S_0 limit, there are only two invariant amplitudes in the forward direction and, as pointed out in Eq. (2.10), the transverse and longitudinal spin-transfer coefficients K_{NN} and K_{LL} are then related by $K_{LL}(0) + 2K_{NN}(0) = -1$. One obvious experimental challenge is to get sufficient energy resolution through the measurement of the produced neutron to guarantee that the residual pp system is in the 1S_0 state. The other general problem is knowing sufficiently well the analysing power of the reaction chosen to measure the final neutron polarisation. Some of the earlier experiments failed on one or both of these counts.

The first measurement of $K_{NN}(0)$ for $d(\vec{p}, \vec{n})pp$ seems to have been performed at the Rochester synchrocyclotron at 200 MeV in the mid-1960s [61]. A neutron polarimeter based upon pn elastic scattering was used, with the analysing power being taken from the existing nucleon–nucleon phase shifts. However, the resolution on the final proton energies was inadequate for our purposes, with an energy spread of 12 MeV FWHM coming from the primary beam and the finite target thickness.

A similar experiment was undertaken at 30 and 50 MeV soon afterwards at the RHEL Proton Linear Accelerator [62]. The results represent averages over the higher momentum part of the neutron spectra. A liquid ^4He scintillator was used to measure the analysing power in neutron elastic scattering from ^4He , though the calibration standard was uncertain by about 8%.

Although falling largely outside the purpose of this review, it should be noted that there were forward angle measurements of $K_{NN}(0)$ at the Triangle Universities Nuclear Laboratory at five very low energies, ranging from 10.6 to 15.1 MeV [63]. This experiment also used a ^4He polarimeter that in addition served to measure the neutron energy with a resolution of the order of 200 keV. Although all the data at the lowest E_{pp} were consistent with $K_{NN}(0) \approx -0.2$, a very strong dependence on the pp excitation energy was found, with $K_{NN}(0)$ passing through zero in all cases for $E_{pp} < 2$ MeV. Hence, after unfolding the resolution it is likely that the true value at $E_{pp} = 0$ is probably slightly more negative than -0.2 . The strong variation with E_{pp} is reproduced in a simple implementation of the Faddeev equations that was carried out, though without the inclusion of the Coulomb interaction [64].

The RCNP experiment at 50, 65, and 80 MeV used a deuterated polyethylene target [65]. The calibration of the neutron polarimetry was on the basis of the charge exchange from ^6Li to the 0^+ ground state of ^6Be , viz $^6\text{Li}(\vec{p}, \vec{n})^6\text{Be}_{\text{gs}}$. Although at the time the polarisation transfer parameters for this reaction had not been measured, they were assumed to be the same as for the transition to the first excited (isobaric analogue) state of ^6Li . This was subsequently shown to be a valid assumption by a direct measurement of neutron production with a ^6Li target [66]. On the other hand, the resolution in E_{pp} was of the order of 6 MeV, which arose mainly from the measurement of the time of flight over 7 m. As a consequence, the authors could not identify clearly the strong dependence of $K_{NN}(0)$ on E_{pp} that was seen in experiments where the neutron energy was better measured [63, 67, 68]. Such a dependence would have been more evident in the data if there had not been a contribution at higher E_{pp} from the ^{12}C in the target.

The most precise measurements of the polarisation transfer parameters at low energies were accomplished in experiments at PSI at 56 and 70 MeV [67, 68]. One of the advantages of their setup was the time structure of the PSI injector cyclotron, where bursts of width 0.7 ns, separated by 20 ns, were obtained at 72 MeV, increasing to about 1.2 ns, separated by 70 ns, at 55 MeV. This allowed the production of a near-monoenergetic neutron beam for use in other low-energy experiments [69]. Beams with a good time structure were also obtained after acceleration of the protons to higher energies and these were necessary for the measurements of $R_{np}(0)$ [31].

The target size was small compared to the time-of-flight path of ≈ 4.3 m in the initial experiment [67] so that the total timing resolution of typically 1.4 ns led to one in E_{pp} of a few MeV. The polarisation of the proton beam was very well known and that of the recoil neutron was measured by elastic scattering of the neutrons from ^4He . Apart from small Coulomb corrections, the analysing power of $^4\text{He}(\vec{n}, n)^4\text{He}$ should be identical to that of the proton in $^4\text{He}(\vec{p}, p)^4\text{He}$, for which reliable data existed.

The results at both 54 and 71 MeV showed that the polarisation transfer parameters change very strongly with the measured neutron energy and hence with E_{pp} . This must go a long way to explain the anomalous results found by the RCNP group [65]. At 54 MeV both K_{NN} and K_{LL} were measured and, when extrapolated to the 1S_0 limit of maximum neutron

energy, the values gave

$$K_{LL} + 2K_{NN} = (-0.1164 \pm 0.013) + 2(-0.4485 \pm 0.011) = -1.013 \pm 0.026, \quad (4.1)$$

in very satisfactory agreement with the 1S_0 identity of Eq. (2.10).

The subsequent PSI measurement at 70.4 MeV made significant refinements in two separate areas [68]. The extension of the flight path to 11.6 m improved the resolution in the neutron energy by about a factor of three, which allowed a much more detailed study to the E_{pp} dependence of K_{NN} to be undertaken. The neutron polarimeter used the $p(\vec{n}, p)n$ reaction, and an independent calibration was carried out by studying the ${}^{14}\text{C}(\vec{p}, \vec{n}){}^{14}\text{N}_{2.31}$ reaction in the forward direction. The 2.31 MeV level in question is the first excited state of ${}^{14}\text{N}$, which is the isospin analogue of the $J^P = 0^+$ ground state of ${}^{14}\text{C}$. In such a case there can be no spin flip and the polarisation of the recoil neutron must be identical to that of the proton beam. In order to isolate this level cleanly, the neutron flight path was increased further to 16.4 m for this target.

The results confirmed those of the earlier experiment [67] and, in particular, showed that even in the forward direction $K_{NN}(0)$ varied significantly with the energy of the detected neutron. The dependence of the parameterisation of the results on E_{pp} is shown in Fig 2. Near the allowed limit, E_{pp} is equal to the deviation of the neutron energy from its kinematically allowed maximum.

A strong variation of the polarisation transfer parameter with E_{pp} is predicted when using the Faddeev equations [68, 70], though these do not give a perfect description of the data. These calculations represent full multiple scattering schemes with all binding corrections and off-shell dependence of the nucleon–nucleon amplitudes. Nevertheless, it is important to note that the $K_{LL}(0)$ prediction for very low E_{pp} is quite close to that of the plane-wave impulse approximation. On the other hand, the fact that both the data and a sophisticated theoretical model show the strong dependence on E_{pp} brings into question the hope that the 1S_0 proton–proton final state remains dominant in the forward direction for low beam energies. This is one more reason to doubt the utility of the Dean sum rule to estimate $R_{np}(0)$ at low energies.

The validity of the plane-wave impulse approximation for the unpolarised $d(p, n)pp$ reaction at 135 MeV has also been tested at IUCF [71]. The conclusions drawn here are broadly similar to those from an earlier study at 160 MeV [72]. In the forward direction the plane-wave approach reproduces the shape of the dependence on E_{pp} out to at least 5 MeV, though the normalisation was about 20% too low. On the other hand, the group evaluated the model using an S -state Hulthén wave function for the deuteron and so it is not surprising that some renormalisation was required. The E_{pp} dependence follows almost exclusively from the pp wave function, which was evaluated realistically. The comparison with more sophisticated

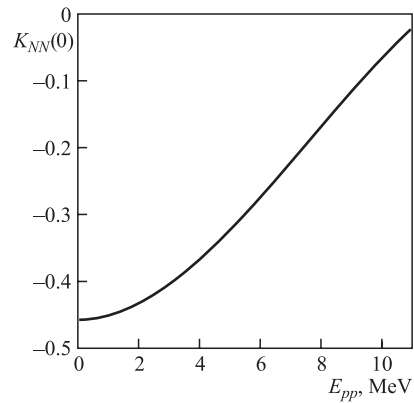


Fig. 2. Fit to the measured values of K_{NN} of the $d(\vec{p}, \vec{n})pp$ reaction in the forward direction at a beam energy of 70.4 MeV as a function of the excitation energy in the pp final state [68]

Table 5. Measured values of the longitudinal and transverse polarisation transfer parameters for the $d(\vec{p}, \vec{n})pp$ reaction in the forward direction. The total estimated uncertainties quoted do not take into account the influence of the different possible choices on the cut on the final neutron momentum. Data marked * have been renormalised to impose $K_{LL}(0) + 2K_{NN}(0) = -0.98$ and the error bar increased slightly

T_N , MeV	$K_{LL}(0)$	$K_{NN}(0)$	Facility	Year	Ref.
10.6	—	-0.17 ± 0.06	TUNL	1980	[63]
12.1	—	-0.20 ± 0.07	TUNL	1980	[63]
13.1	—	-0.14 ± 0.05	TUNL	1980	[63]
14.1	—	-0.12 ± 0.06	TUNL	1980	[63]
15.1	—	-0.22 ± 0.09	TUNL	1980	[63]
30	—	-0.13 ± 0.03	RHEL	1969	[62]
50	—	-0.23 ± 0.07	RHEL	1969	[62]
50	—	-0.27 ± 0.05	RCNP	1986	[65]
54	-0.116 ± 0.013	-0.449 ± 0.011	PSI	1990	[67]
65	—	-0.31 ± 0.03	RCNP	1986	[65]
70.4	—	-0.457 ± 0.011	PSI	1999	[68]
71	—	-0.480 ± 0.013	PSI	1990	[67]
80	—	-0.37 ± 0.04	RCNP	1986	[65]
160	—	-0.43 ± 0.04	IUCF	1987	[72]
203	—	-0.27 ± 0.11	Rochester	1987	[61]
305	-0.411 ± 0.010	—	LAMPF	1992	[73]
318	-0.41 ± 0.01	—	LAMPF	1993	[75]
485	-0.579 ± 0.011	—	LAMPF	1992	[73]
494	-0.59 ± 0.01	—	LAMPF	1993	[75]
500	$-0.60 \pm 0.03^*$	$-0.19 \pm 0.04^*$	LAMPF	1985	[18]
635	-0.686 ± 0.012	—	LAMPF	1992	[73]
650	$-0.79 \pm 0.03^*$	$-0.10 \pm 0.03^*$	LAMPF	1985	[18]
722	-0.717 ± 0.013	—	LAMPF	1992	[73]
788	-0.720 ± 0.017	—	LAMPF	1992	[73]
800	$-0.68 \pm 0.05^*$	$-0.15 \pm 0.04^*$	LAMPF	1981	[17]
800	$-0.78 \pm 0.04^*$	$-0.10 \pm 0.04^*$	LAMPF	1985	[18]

Faddeev calculations was, of course, hampered by the difficulty of including the Coulomb interaction, which is particularly important for low E_{pp} [14].

The values of $K_{NN}(0)$ obtained at IUCF at 160 MeV [72] show a weaker dependence on E_{pp} than that found in the experiments below 100 MeV [67, 68]. Nevertheless, these data do indicate that the influence of P waves in the final pp system is not negligible for $E_{pp} \approx 10$ MeV.

The early measurements of $K_{NN}(0)$ and $K_{LL}(0)$ at LAMPF [17, 18] were hampered by the poor knowledge of the neutron analysing power in $\vec{n}p$ elastic scattering that was used in the polarimeter. This was noted by Bugg and Wilkin [13], who pointed out that, although the data were taken in the forward direction and with good resolution, they failed badly to satisfy the identity of Eq. (2.10). They suggested that both polarisation transfer parameters should be renormalised by overall factors so as to impose the condition. In view of this argument and the results of the subsequent LAMPF experiment [73], the values reported from these

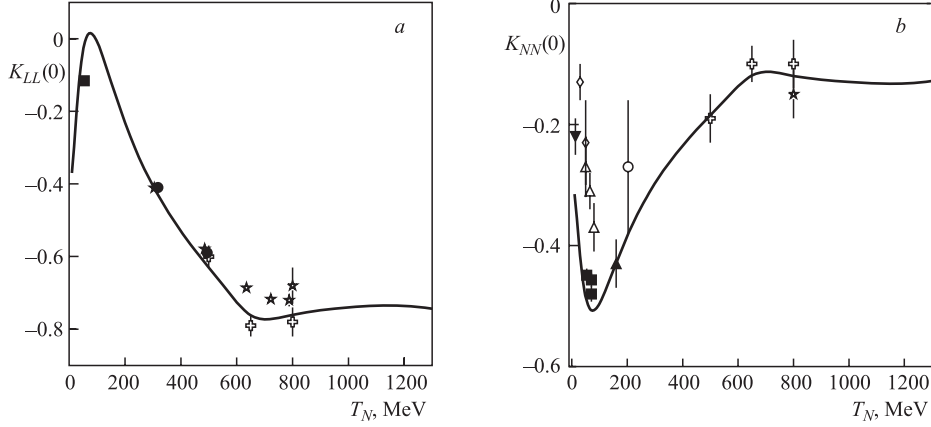


Fig. 3. Forward values of the longitudinal and transverse polarisation transfer parameters: $K_{LL}(0)$ (a) and $K_{NN}(0)$ (b) in the $d(\vec{p}, \vec{n})pp$ reaction as functions of the proton kinetic energy T_N . In general we believe that greater confidence can be placed in the data represented by closed symbols, which are from [73] (stars), [75] (circles), [72] (triangle), [67, 68] (squares), and the average of the five TUNL low energy points [63] (inverted triangle). The open symbols come from [62] (diamonds), [65] (triangle), [61] (circle), [18] (crosses), and [17] (star), with the latter two being renormalised as explained in Table 5. The curve is the plane wave 1S_0 prediction of Eq. (2.8), as tabulated in Table 1

experiments in Table 5 have been scaled such that $K_{LL}(0) + 2K_{NN}(0) = -0.98$ (to allow for some dilution from the P waves in the pp system) and the error bars increased a little to account for the uncertainty in this procedure.

The above controversy regarding the values of the forward polarisation transfer parameters in the 500–800 MeV range was conclusively settled by a subsequent LAMPF experiment by McNaughton et al. in 1992 [73]. Following an idea suggested by Bugg [74], the principle was to produce a polarised neutron beam through the $d(\vec{p}, \vec{n})pp$ reaction, sweep away the charged particles with a bending magnet, and then let the polarised neutron beam undergo a second charge exchange through the $d(\vec{n}, \vec{p})nn$ reaction. By charge symmetry, the values of $K_{LL}(0)$ for the two reactions are the same and, if the energy loss in both cases is minimised, the beam polarisation P_b and final proton polarisation P_p are related by

$$P_p = [K_{LL}(0)]^2 P_b. \quad (4.2)$$

The beauty of this technique is that only proton polarisations had to be measured with different but similarly calibrated instruments. Also, because the square occurs in Eq. (4.2), the errors in the evaluation of K_{LL} are reduced by a factor of two. The energy losses were controlled by time-of-flight measurements, and very small corrections were made for the fact that the two reactions happened at slightly different beam energies.

The overall precision achieved in this experiment was typically 3%, and the results clearly demonstrated that there had been a significant miscalibration in much of the earlier LAMPF neutron polarisation standards. The group also suggested clear renormalisations of the measured polarisation transfer parameters. Since several of the authors of the earlier papers also signed the McNaughton work, this lends a seal of approval to the procedure.

The longitudinal polarisation transfer in the forward direction was measured later at LAMPF at 318 and 494 MeV [75] with neutron flight paths of, respectively, 200 and 400 m so that the energy resolution was typically 750 keV (FWHM). This allowed the authors to use the $^{14}\text{C}(\vec{p}, \vec{n})^{14}\text{N}_{2.31}$ reaction to calibrate the neutron polarimeter, a technique that was taken up afterwards at PSI [68]. Including these results, we now have reliable values of either $K_{LL}(0)$ or $K_{NN}(0)$ from low energies up to 800 MeV.

4.1. Data Summary. The values of $K_{NN}(0)$ and $K_{LL}(0)$ measured in the experiments discussed above are presented in Table 5 and shown graphically in Fig. 3. The results are compared in the figure with the predictions tabulated in Table 1 of the pure 1S_0 plane-wave impulse approximation of Eq. (2.9) that used the SAID phase shifts [22] as input. Wherever possible the data are extrapolated to $E_{pp} = 0$. This is especially important at low energies and, if this causes uncertainties or there are doubts in the calibration standards, we have tried to indicate such data with open symbols, leaving closed symbols for cases where we believe the data to be more trustworthy.

The impulse approximation curve gives a semi-quantitative description of all the data, especially the more «reliable» results. At low energies we expect that this approach would be at best indicative but it is probably significant that the curve falls below the McNaughton et al. results [73] in the 500 to 800 MeV range, where the approximation should be much better. It is doubtful whether the Glauber correction [13, 60] can make up this difference, and this suggests that the current values of the SAID neutron–proton charge-exchange amplitudes [22] might require some slight modifications in this energy region. Similar evidence is found from the measurements of the deuteron analysing power, to which we now turn.

5. DEUTERON POLARISATION STUDIES IN HIGH-RESOLUTION ($\vec{d}, 2p$) EXPERIMENTS

We have pointed out through Eq. (2.12) that in the 1S_0 limit the deuteron ($\vec{d}, 2p$) tensor analysing power in the forward direction can be directly evaluated in terms of the (\vec{p}, \vec{n}) polarisation transfer coefficient. Therefore, instead of measuring beam and recoil polarisations, much of the same physics can be investigated by measuring the analysing power with a polarised deuteron beam without any need to detect the polarisation of the final particles. This is the approach advocated by Bugg and Wilkin [13, 19]. Unlike the sum-rule methodology applied by a Dubna group [47], only the small part of the $p(\vec{d}, 2p)n$ final phase space where E_{pp} is at most a few MeV needs to be recorded. For this purpose, one does not need the large acceptance offered by a bubble chamber and four separate groups have undertaken major programmes using different electronic equipment. We now discuss their results.

5.1. The SPES IV Experiments. The Franco-Scandinavian collaboration working at Saclay studied the $p(\vec{d}, 2p)n$ reaction at 0.65, 1.6, and 2.0 GeV by detecting both protons in the high-resolution SPES IV magnetic spectrometer [76–79]. The small angular acceptance ($1.7 \times 3.4^\circ$) combined with a momentum bite of $\Delta p/p \approx 7\%$ gave access only to very low pp excitation energies, and Monte Carlo simulations showed that the peak of the E_{pp} distribution was around 650 keV. Under these circumstances any contamination from P waves in the pp system can be safely neglected. On the other hand, the small angular acceptance meant that away from the forward direction the data were primarily sensitive to A_{NN} . On account of

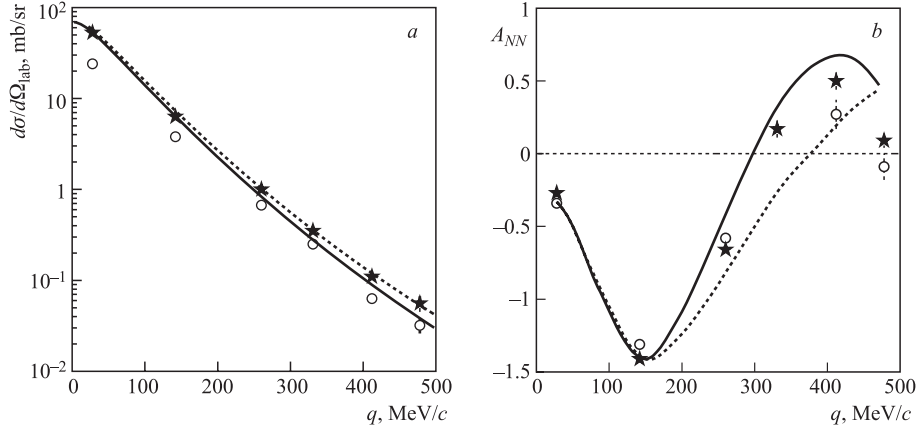


Fig. 4. The measurements of the $p(\bar{d}, 2p)n$ laboratory differential cross section (a) and deuteron tensor analysing power (b) at 1.6 GeV by the Franco-Scandinavian group [79] are compared to their theoretical impulse approximation estimates without the double scattering correction (dashed curve) and with (solid line). The experimental cross section data (stars) have been normalised to the solid line at $q = 0.7 \text{ fm}^{-1}$. It should be noted that the ratio of the data on deuterium (open circles) to those on hydrogen is not affected by this uncertainty

the small acceptance, the deflection angle in the spectrometer was adjusted to measure the differential cross section and A_{NN} at discrete values of the momentum transfer q .

The results for the laboratory differential cross section and A_{NN} obtained at 1.6 GeV for both the $p(\bar{d}, 2p)n$ and quasi-free $d(\bar{d}, 2p)nn$ reactions are shown in Fig. 4. Also shown in the figure are the authors' theoretical predictions of the plane-wave impulse approximation and also ones that included the Glauber double-scattering term [13, 60]. These give quite similar results for momentum transfers below about 150 MeV/c but produce important changes for larger q , especially in the deuteron analysing power. The neutron-proton charge-exchange amplitudes used were the updated versions of the analysis given in [80] that were employed in other theoretical estimates [13, 81–83]. The predictions were averaged over the SPES IV angular acceptance and, in view of the rapid change in the transition form factor with q , this effect can be significant. The validity of this procedure was tested by reducing the horizontal acceptance by a factor of two [78].

The acceptance of the SPES IV spectrometer for two particles was very hard to evaluate with any precision, and the hydrogen data were normalised to the theoretical prediction at $q = 0.7 \text{ fm}^{-1}$ that included the Glauber correction. On the other hand, the ratio of the cross section with a deuterium and hydrogen target could be determined absolutely and, away from the forward direction, was found to be 0.68 ± 0.04 . This is reduced even more for small q , precisely because of the Pauli blocking in the unobserved nn system, similar to that we discussed for the evaluation of $R_{np}(0)$. Since for small E_{pp} the np spin-independent amplitude cannot contribute and the spin-orbit term vanishes at $q = 0$, the extra reduction factor should be precisely $2/3$, which is consistent with the value observed.

A high-precision (unpolarised) $d(d, 2p)nn$ experiment was undertaken at KVI (Groningen) to investigate the neutron-neutron scattering length [84]. In this case, the pp and nn systems

were both in the 1S_0 region of very small excitation energies. The shape of the nn excitation energy spectrum was consistent with that predicted by plane-wave impulse approximation with reasonable values of the nn scattering length.

The primary aim of the Franco-Scandinavian group was the investigation of spin-longitudinal and transverse responses in medium and heavy nuclei and also to extend these studies to the region of $\Delta(1232)$ excitation in the $\vec{d}p \rightarrow \{pp\}\Delta^0$. Nevertheless, it is interesting to ask how useful these data could be for the establishment or checking of neutron-proton observables. The $(d, 2p)$ transition form factor decreases very rapidly with momentum transfer because of the large deuteron size. As a consequence, the Glauber double scattering term, which shares the momentum transfer between two collisions, becomes relatively more important. Estimates of this effect are more model-dependent [13, 79] and, as is seen from Fig. 4, it may be dangerous to rely on them beyond about $q \approx 150$ MeV/ c .

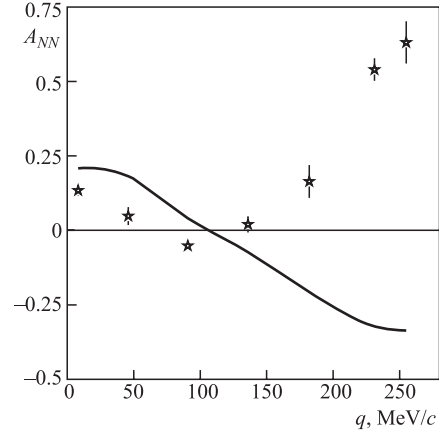
Absolute cross sections were not measured in these experiments, and there were only two points in the safe region of momentum transfer and these represented averages over significant ranges in q . The central values of q marked in Fig. 4 were evaluated from a Monte Carlo simulation of the spectrometer that used the theoretical model as input. As a consequence, the results give relatively little information on the magnitudes of the spin-flip compared to the non-spin-flip amplitudes. It is perhaps salutary to note that at larger q the estimate of the cross section without the double scattering correction describes the data better than that which included it. However, the reverse is true for the analysing power.

The major contribution to the np database comes from the measurement of A_{NN} at small q . Since the beam polarisation was known with high precision, this provides a robust relation between the magnitudes of the three spin-flip amplitudes but only at two average values of q . Neutron-proton scattering has been extensively studied in the 800 MeV region [22], and so it is not surprising that this $p(\vec{d}, 2p)n$ experiment gave results that are completely consistent with its predictions. The dip in A_{NN} in both the theoretical estimates and the experimental data is due primarily to the expected vanishing of the distorted one-pion-exchange contribution to one of the spin-spin amplitudes for $q \approx m_\pi$.

5.2. The RCNP Experiments. Almost simultaneously with the start of the SPES IV experiments [76], an RCNP group studied the deuteron tensor analysing power A_{NN} in the $p(\vec{d}, 2p)n$ reaction at a much lower energy of $T_d = 70$ MeV [85]. The primary motivation was to compare the forward angle data with the results of the polarisation transfer parameter K_{NN} that had been measured previously by the same group [65]. For small angles a magnetic spectrograph was used, which restricted the excitation energy of the final protons to be less than 200 keV. At larger angles, where the cross section is much smaller, a Si telescope array with a larger acceptance was employed and the selection $E_{pp} < 1$ MeV was imposed in the off-line analysis. In all cases, the only significant background arose from the random coincidence of two protons from the breakup of separate deuterons. This is particularly important for small angles due to the spectator momentum distribution in the deuteron. Additional data were taken at 56 MeV, but solely in the forward direction.

At such low energies, the plane-wave impulse approximation based upon the neutron-proton charge-exchange amplitudes may provide only a semi-quantitative description of the experimental data; there are likely to be significant contributions from direct diagrams. Nevertheless, as can be seen in Fig. 5, the estimates given in the paper [85] that were made using the then existing (SP86) SAID phase shift solution [22] were reasonable near the forward direction and would be even closer if modern np solutions were used. At larger

Fig. 5. Measurements of the deuteron tensor analysing power A_{NN} for the $p(\vec{d}, 2p)n$ reaction at $T_d = 70$ MeV by the RCNP collaboration as a function of momentum transfer q [85]. In all cases $E_{pp} < 1$ MeV. The results are compared to the authors' own theoretical plane-wave impulse approximation estimates that were based upon the SAID SP86 phase shift solution [22]



angles there is significant disagreement between the data and model and the authors show that part of this could be rectified if the np input amplitudes were evaluated at the mean of the incident and outgoing energies. This feature has been implemented in the more refined impulse approximation calculations of [81], where the theory was evaluated in the brick-wall frame.

The group was disappointed to find that in the forward direction the relation of Eq. (2.12) between their own (\vec{p}, \vec{n}) spin transfer data [65] and their deuteron tensor analysing power was far from being satisfied. This could not be explained by the difference in beam energy or the smearing over small angles. Because the $(d, 2p)$ results were obtained under the clean 1S_0 conditions of $E_{pp} < 200$ keV, the problem must be laid at the door of the much poorer energy resolution associated with the detection of neutrons. It was only the later PSI experiment [68] which showed that the spin-transfer parameter varied very strongly with E_{pp} and, as argued in Sec. 4, this is probably the resolution of the discrepancy.

5.3. The EMRIC Experiments. The aims and the equipment of the EMRIC collaboration [81–83], also working at Saclay, were very different and much closer to the original ideas of Bugg and Wilkin [13, 19]. The driving force was the desire to use the $(\vec{d}, 2p)$ reaction as the basis for the construction of a deuteron tensor polarimeter that could be used to measure the polarisation of the recoil deuteron in electron–deuteron elastic scattering. For this purpose the device had to have a much larger acceptance than that available at SPES IV and be compact, so that it could be transported to and implemented in experiments at an electron machine.

The EMRIC apparatus was composed of an array of 5×5 CsI scintillator crystals ($4 \times 4 \times 10$ cm), optically coupled to phototubes, which provided information on both energy and particle identification. Placed at 70 cm from the liquid hydrogen target, it subtended an angular range of $\pm 7^\circ$ so that several overlapping settings were used in order to increase the angular coverage. Since the orientation of the deuteron polarisation could be rotated through the use of a solenoid, away from the forward direction this gave access to both transverse deuteron tensor analysing powers, the sideways A_{SS} as well as the normal A_{NN} , under identical experimental conditions.

In the initial experiment at a deuteron beam energy of $T_d = 200$ MeV [82], the angular resolution achieved with the CsI crystals was only $\pm 1.6^\circ$ but in the second measurement at $T_d = 350$ MeV the system was further equipped with two multiwire proportional chambers

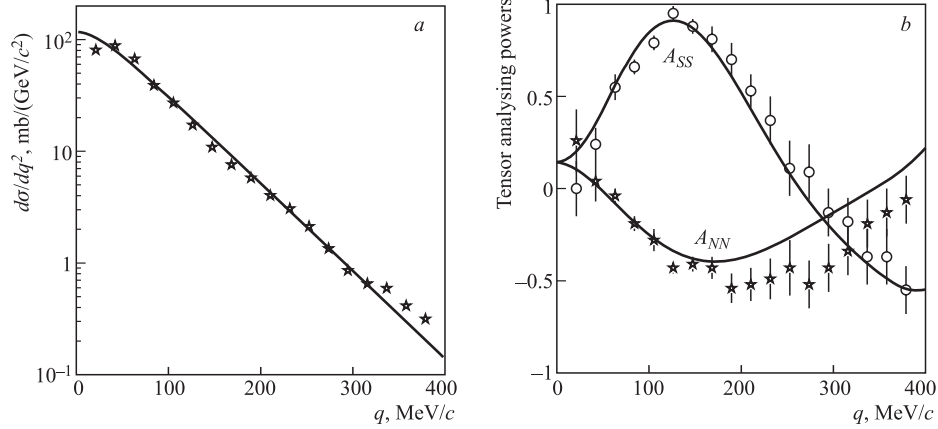


Fig. 6. Measurements of the $p(\vec{d}, 2p)n$ differential cross section (a) and two deuteron tensor analysing powers (b) for $E_{pp} < 1$ MeV at a beam energy of $T_d = 350$ MeV by the EMRIC collaboration [83] are compared to the theoretical plane-wave impulse approximation estimates of [81]. The values of both the experimental cross section data and theoretical model have been scaled up by a factor of two to correct a presentational oversight in the publication [83]

that improved it to 0.1° . Having identified fast protons using a pulse-shape analysis technique based on the time-decay properties of the CsI crystals, their energies could be measured with a resolution of the order of 2%. The missing mass of a proton pair yielded a clean neutron signal with a $\text{FWHM} = 14$ MeV/c^2 , the only contamination coming from events where not all the energy was deposited in the CsI array.

The compact system allowed measurements over the wide angular and E_{pp} ranges that are necessary for the construction of a polarimeter with a high figure of merit. However, for the present discussion we concentrate our attention purely on the data where $E_{pp} < 1$ MeV, for which the dilution of the analysing power signal by the proton–proton P waves is small. The EMRIC results for the differential cross section and two tensor analysing powers at 350 MeV are shown in Fig. 6. Due to a slip in the preparation of the publication [83], both the experimental data and the impulse approximation model were downscaled by a factor of two [86], which has been corrected in the figure shown here. One should take into account that there are systematic errors (not shown) arising from the efficiency corrections that are estimated to be typically of the order of 20%, though they are larger at the edges of EMRIC [87]. This might account for the slight oscillations of the data around the theoretical prediction in Fig. 6.

The plane-wave impulse approximation calculation of [81] describes the data quite well, though one has to note that the presentation is on a logarithmic scale and that there are at least 20% normalisation uncertainties. The data represented three settings of the EMRIC facility, and their fluctuations around the predictions could be partially due to minor imperfections in the acceptance corrections. The model is also satisfactory for the analysing powers out to at least $q \approx 150$ MeV/c , from which point the A_{NN} data remain too negative. However, as we argued with the SPES IV results of Fig. 4, it is at about this value of q that the Glauber double scattering correction becomes significant. We can therefore conclude that the good

agreement of the A_{SS} and A_{NN} data in the «safe» region of $q \lesssim 150$ MeV/ c is confirmation that the ratios of the different spin–spin contributions given by the Bugg amplitudes of [80] are quite accurate. Nevertheless, their overall strength is checked far less seriously by these data because of the normalisation uncertainty and the logarithmic scale of Fig. 4.

The EMRIC experiment [83] was the only one of those discussed that was capable of investigating the variation of the deuteron analysing power A_{NN} with excitation energy and, in view of the strong effects found for the $d(\vec{p}, \vec{n})pp$ polarisation transfer parameters at 56 and 70 MeV [67, 68], it would be interesting to see if anything similar happened for A_{NN} . Extrapolating the $T_d = 200$ MeV results to the forward direction, it is seen that $A_{NN} \approx 0.23, 0.17,$ and 0.10 for the three bins of excitation energy $E_{pp} < 1$ MeV, $1 < E_{pp} < 4$ MeV, and $4 < E_{pp} < 8$ MeV, respectively. This variation is smaller than that found for K_{NN} [67, 68]. On the other hand, since the (longitudinal) momentum transfer remains very small in the forward direction, the plane-wave impulse approximation predicts very little change with E_{pp} .

The aim of the group was to show that the $(\vec{d}, 2p)$ reaction had a large and well-understood polarisation signal, and this was successfully achieved. The experience gained with the EMRIC device laid the foundations for the development of the POLDER polarimeter [86, 88], which was subsequently used to separate the contributions from the deuteron monopole and quadrupole form factors at JLab [89].

5.4. The ANKE Experiments. A fourth experimental approach is currently being undertaken using the ANKE magnetic spectrometer that is located at an internal target position forming a chicane in the COSY (COoler SYnchrotron). This machine is capable of accelerating and storing protons and deuterons with momenta up to 3.7 GeV/ c , i.e., kinetic energies of $T_p = 2.9$ GeV and $T_d = 2.3$ GeV. The $(\vec{d}, 2p)$ measurements form part of a much larger spin programme that will use combinations of polarised beams and targets [90]. Only results from a test experiment at $T_d = 1170$ MeV are presently available [91, 92], and these are described below.

There are several problems to be overcome before the $p(\vec{d}, 2p)n$ reaction could be measured successfully at ANKE. The horizontal acceptance for the reaction is limited to laboratory angles in the range of approximately $-2^\circ < \theta_{\text{hor}} < 4^\circ$ and much less in the vertical direction. This constrains severely the range of momentum transfers that can be studied. Furthermore, the axis of the spin alignment of the circulating beam is vertical and, unlike the EMRIC case [83], there is insufficient place for a solenoid to rotate the polarisation. As a consequence, the values of A_{NN} and A_{SS} cannot be extracted under identical conditions. Furthermore, the polarisations of the beam have to be checked independently at the ANKE energy. Finally, unlike the external beam experiments of SPES IV or EMRIC, the luminosity inside the storage ring has also to be established at the ANKE position.

Most of the above difficulties can be addressed by using the fact that one can observe and measure simultaneously in ANKE the following reactions: $\vec{d}p \rightarrow \{pp\}n$, $\vec{d}p \rightarrow dp$, $\vec{d}p \rightarrow {}^3\text{He}\pi^0$, and $\vec{d}p \rightarrow p_{\text{sp}}d\pi^0$, where p_{sp} is a fast spectator proton. What cannot, of course, be avoided is the cut in the momentum transfer which at $T_d = 1170$ MeV means that the deuteron charge-exchange reaction has good acceptance only for $q \lesssim 150$ MeV/ c . However, we already saw in the SPES IV case that for larger momentum transfers the double scattering corrections become important and, as a result, the extraction of information on np amplitudes becomes far more model-dependent.

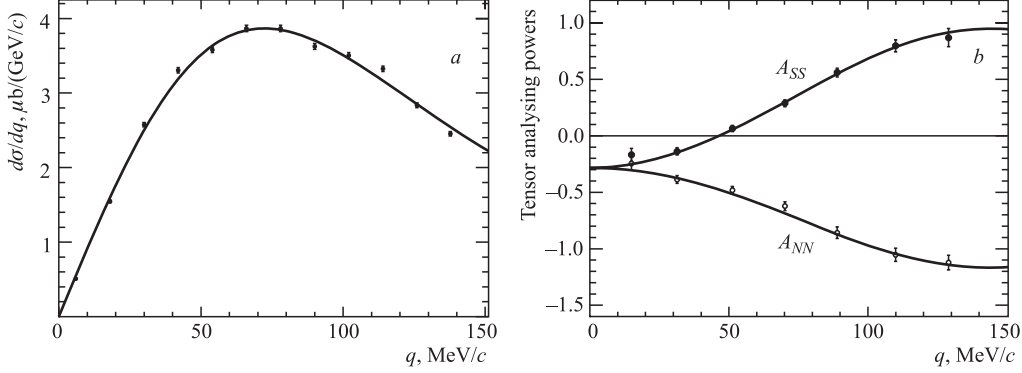


Fig. 7. Measurements of the $p(\vec{d}, 2p)n$ differential cross section (a) and two deuteron tensor analysing powers (b) for $E_{pp} < 1$ MeV at a beam energy of $T_d = 1170$ MeV by the ANKE collaboration [91,92] are compared to the theoretical plane-wave impulse approximation estimates of [81]

The luminosity, and hence the cross section, was obtained from the measurement of the $dp \rightarrow p_{sp}d\pi^0$ reaction, for which the final spectator proton and produced deuteron fall in very similar places in the ANKE forward detector to the two protons from the charge-exchange reaction. Using only events with small spectator momenta and interpreting the reaction as being due to that induced by the neutron in the beam deuteron, $np \rightarrow d\pi^0$, reliable values could be obtained for the luminosity. This approach had the subsidiary advantage that to some extent the Glauber shadowing correction [60] cancels out between the $dp \rightarrow p_{sp}d\pi^0$ and $dp \rightarrow \{pp\}n$ reactions.

The COSY polarised ion source that feeds the circulating beam was programmed to provide a sequence of one unpolarised state, followed by seven combinations of deuteron vector and tensor polarisations. Although these were measured at low energies, it had to be confirmed that there was no loss of polarisation through the acceleration up to $T_d = 1170$ MeV. This was done by measuring the analysing powers of $\vec{d}p \rightarrow dp$, $\vec{d}p \rightarrow {}^3\text{He}\pi^0$, and $\vec{d}p \rightarrow p_{sp}d\pi^0$ and comparing with results given in the literature [93]. As expected, there was no discernable depolarisation.

Due to the geometric limitations, the acceptance of the ANKE forward detector varies drastically with the azimuthal production angle ϕ . The separation between A_{NN} and A_{SS} depends upon studying the variation of the cross section with ϕ . An accurate knowledge of the acceptance is not required for this purpose because one can work with the ratio of the polarised to unpolarised cross section where, to first order, the acceptance effects drop out. The Monte Carlo simulation of the acceptance was sufficiently good to give only a minor contribution to the error in the unpolarised cross section itself. The claimed overall cross section uncertainty of 6% is dominated by that in the luminosity evaluation.

The limited ANKE acceptance also cuts into the E_{pp} spectrum and the collaboration only quote data integrated up to a maximum of 3 MeV. The results shown in Fig. 7 were obtained with a cut of $E_{pp} < 1$ MeV, as were the updated theoretical predictions from [81], where the current SAID np elastic amplitudes at 585 MeV were used as input [22].

The agreement between the plane-wave impulse approximation and the experimental data is very good for all three observables over the full momentum transfer range that is accessible

Table 6. Measured values of the forward deuteron tensor analysing power A_{NN} in the $\vec{d}p \rightarrow \{pp\}n$ reaction in terms of the kinetic energy per nucleon T_N . The errors include some estimate for the extrapolation to $\theta = 0^\circ$

T_N , MeV	$A_{NN}(0)$	Facility	Year	Ref.
28	0.015 ± 0.021	RCNP	1987	[85]
35	0.134 ± 0.018	RCNP	1987	[85]
100	0.23 ± 0.03	EMRIC	1993	[83]
175	0.15 ± 0.03	EMRIC	1993	[83]
325	-0.05 ± 0.03	SPES IV	1995	[79]
585	-0.26 ± 0.03	ANKE	2009	[92]
800	-0.27 ± 0.04	SPES IV	1995	[79]
1000	-0.32 ± 0.04	SPES IV	1995	[79]

at ANKE. Since there have been many neutron–proton experiments in this region, it is to be believed that the np elastic scattering amplitudes are very reliable at 585 MeV. Extrapolating the results to $q = 0$ and using the impulse approximation model, one finds that $A_{NN} = -0.26 \pm 0.02$. This is to be compared to the SAID value of -0.28 , though no error can be deduced directly on their prediction [22]. All this suggests that the methodology applied by the ANKE collaboration is sufficient to deliver useful np amplitudes at higher energies, where less is known experimentally. Compared to the SPES IV and EMRIC experiments, there are finer divisions in momentum transfer and hence more points in the safe q region.

Apart from taking data up to a maximum COSY energy of $T_d \approx 2.3$ GeV, there are plans to measure the deuteron charge-exchange reaction with a polarised beam and target [90]. The resulting values of the two transverse spin correlation parameters will allow the relative phases of the spin-flip amplitudes to be determined.

To go higher in energy, it will be necessary to use a proton beam on a deuterium target, detecting both slow recoil protons from the $p\vec{d} \rightarrow \{pp\}n$ in the silicon tracking telescopes with which ANKE is equipped [94]. The drawback here is that the telescopes require a minimum momentum transfer so that the energies of the protons can be measured and this is of the order of 150 MeV/c at low E_{pp} . This technique has already been used at CELSIUS to generate a tagged neutron beam on the basis of the $pd \rightarrow npp$ reaction at 200 MeV by measuring both slow recoil protons in silicon microstrip detectors [95].

5.5. Data Summary. In Table 6 we present the experimental values of the deuteron tensor analysing power in the $\vec{d}p \rightarrow \{pp\}n$ reaction extrapolated to the forward direction. The error bars include some attempt to take into account the uncertainty in the angular extrapolation. The resulting data are also shown in Fig. 8.

In the forward direction the plane-wave impulse approximation predictions of Eq. (2.8) for the forward analysing power should be quite accurate provided that the excitation energy in the final diproton is small so that it is in the 1S_0 state. This condition is well met by the data described here, where E_{pp} is always below 1 MeV [79, 83, 85, 92]. This prediction, which is also tabulated in Table 1, describes the trends of the data very well in regions where the neutron–proton phase shifts are well determined.

We also show in the figure the values of A_{NN} deduced using Eq. (2.12) from the $d(\vec{p}, \vec{n})pp$ measurements summarised in Table 5. Only those data are retained where the neutron

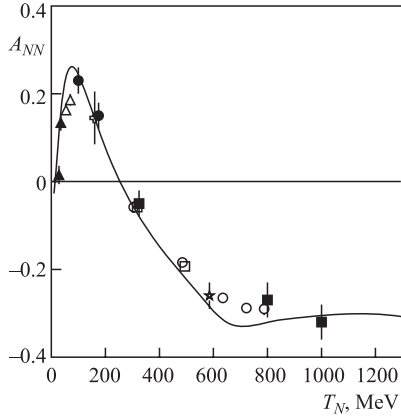


Fig. 8. Values of the forward deuteron tensor analysing power in the $\vec{d}p \rightarrow \{pp\}n$ reaction as a function of the kinetic energy per nucleon T_N . The directly measured experimental data (closed symbols) from SPES IV (squares) [79], EMRIC (circles) [83], ANKE (star) [92], and RCNP (triangles) [85] were all obtained with a pp excitation energy of 1 MeV or less. The error bars include some estimate of the uncertainty in the extrapolation to $\theta = 0$. The open symbols were obtained from measurements of the polarisation transfer parameter in $d(\vec{p}, \vec{n})pp$ by using Eq. (2.12). The data are from [73] (circles), [75] (squares), [72] (cross), and [67, 68] (triangles). The curve is the plane wave 1S_0 prediction of Eq. (2.8), as tabulated in Table 1

polarisation was well measured and the pp excitation energy was small, though generally not as well determined as when the two final protons were detected. The consistency between the (\vec{d}, pp) and (\vec{p}, \vec{n}) data is striking and it is interesting to note that they both suggest values of A_{NN} that are slightly lower in magnitude at high energies than those predicted by the np phase shifts of the SAID group [22]. The challenge now is to continue measuring these data into the more uncharted waters of even higher energies.

Although we have concentrated here on the results for the forward analysing power, it is clear that this represents only a small part of the total data set as demonstrated by the results of Figs. 4, 6, and 7.

6. CONCLUSIONS

Originally the deuteron was thought of merely as a useful substitute for a free neutron target. As an example of this, it has been shown that at large momentum transfers the spin-dependent parameters measured in free np scattering and quasi-free in pd collisions give very similar results [24]. The situation is very different at low momentum transfers where it is not clear which of the nucleons is the spectator or, indeed, whether the concept of calling one of the nucleons a spectator makes any sense at all. However, a more interesting effect comes about in the medium-energy neutron charge exchange on the deuteron, $nd \rightarrow p\{nn\}$, when the excitation energy E_{nn} in the two-neutron system is very low. Under such conditions the Pauli principle demands that the two neutrons should be in a 1S_0 state and there then has to be spin-flip isospin-flip transition from the spin-triplet np in the deuteron to the singlet nn system. The rate for the charge-exchange deuteron breakup $nd \rightarrow p\{nn\}$ would then depend primarily on the spin-spin $np \rightarrow pn$ amplitudes.

The above remarks only assume a practical importance because of an «accident» in the low-energy nucleon–nucleon interaction. In the nn system there is an antibound (or virtual) state pole only a fraction of an MeV below threshold. Although the pole position is displaced slightly in the pp case by the Coulomb repulsion, it results in huge pp and nn scattering lengths. In the $nd \rightarrow pnn$ reaction, it leads to the very characteristic peak at the hard end of the momentum spectrum of the produced proton. Since we know that these events are the result of the spin-flip interaction, we clearly want to use them to investigate in greater depth

this interaction. There are two distinct ways to try to achieve our aims and we have tried to review them both in this article. These are the inclusive (sum-rule) approach of Sec. 3 and the high-resolution polarisation experiments of Secs. 4 and 5.

In impulse approximation, at zero momentum transfer, the $d(n,p)nn$ interaction only excites spin-singlet final states, and Dean [11,12] has shown that the inclusive measurement of the proton momentum spectrum can then be interpreted in terms of the spin-flip np amplitudes through the use of a sum rule. Though the shape of the proton momentum spectrum must depend upon the details of the low-energy nn interaction and also on the deuteron D state, the integral over all momenta would not, provided that the sum rule has converged before any of the limitations imposed by the three-body phase space have kicked in.

The inclusive approach has many positive advantages, in addition to being independent of the low-energy nucleon–nucleon dynamics. In a direct comparison of the production rates of protons in the $d(n,p)nn$ and $p(n,p)n$ reactions using the same apparatus, many of the sources of systematic errors drop out in the evaluation of the cross section ratio $R_{np}(0)$. These are primarily effects associated with the neutron flux and uncertainties in the proton detection system.

There are, however, no similar benefits when working with a proton beam, where one measures instead $d(p,n)pp$. Here one can only construct the $R_{pn}(0)$ ratio by dividing by a $p(n,p)n$ cross section that has been measured in an independent experiment. This is probably the reason why there are fewer entries in Table 3 compared to Table 2. We must therefore stress that, in general, the $d(np)nn$ determinations of $R_{np}(0)$ are much to be preferred over those of $d(p,n)pp$.

On the face of it, the determination of $R_{pn}(0)$ through the measurement of the two fast protons from the $p(d,pp)n$ reaction in a bubble chamber looks like a very hard way to obtain a result [47]. In addition to having to use independent data to provide the normalisation cross section in the denominator, the reaction is first measured exclusively in order afterwards to construct an inclusive distribution. On the other hand, a full kinematic determination allows one to check many of the assumptions made in the analysis and, in particular, those related to the isolation of the charge-exchange impulse approximation contribution from those of other possible Feynman diagrams.

A major difficulty in any of the inclusive measurements is ensuring that the phase space is sufficiently large that the sum rule has been saturated without being contaminated by other driving mechanisms. This means that the low-energy determinations of $R_{np}(0)$ are all likely to underestimate the «true» value and there could be some effects from this even through the energy range of the PSI experiments [31]. Even more worrying is the fact that at low energies the rapid variation of $K_{NN}(0)$ with E_{pp} , as measured in the $d(\vec{p},\vec{n})pp$ reaction [68], shows that there are significant deviations from plane-wave impulse approximation with increasing E_{pp} . These deviations are probably too large to be ascribed to effects arising from the variation of the longitudinal momentum transfer with E_{pp} . This brings into question the whole sum rule approach at low energies.

The alternative high-resolution approach of measuring the 1S_0 peak of the final-state interaction requires precisely that, i.e., high resolution. This can be achieved in practice by measuring the (n,p) reaction with a very long time-of-flight path [75] or by measuring the protons in the $dp \rightarrow \{pp\}n$ reaction with either a deuteron beam [79, 83, 92] or a very low density deuterium target [46]. The resulting data are then sensitive to the low-energy np interaction in the deuteron and the pp interaction in the 1S_0 final state. However,

such interactions are well understood and lead to few ambiguities in the charge-exchange predictions. Establishing a good overall normalisation can present more of a challenge. In addition to obvious acceptance and efficiency uncertainties, if one evaluates a cross section integrated up to say $E_{pp} = 3$ MeV then one has to measure the 3 MeV with good absolute precision, which is non-trivial for a deuteron beam in the GeV range. Hence it might be that at high energies the inclusive measurements could yield more precise determinations of absolute values of $R_{np}(0)$ [41] than could be achieved by using high-resolution experiments.

On the other hand, measuring just the FSI peak with good resolution allows one more easily to follow the variation with momentum transfer and there are also fewer kinematic ambiguities. More crucially, the spin information from the (\vec{n}, \vec{p}) or $(\vec{d}, \{pp\})$ reactions enables one to separate the different spin contributions to the small-angle charge-exchange cross section. It could of course be argued that this is not just a benefit for an exclusive reaction since, if the Dubna bubble chamber experiments [47] had been carried out with a polarised deuteron beam, then these would also have been able to separate the contributions from the two independent forward spin–spin contributions through the use of the generalised Dean sum rule [10, 13]. It is, however, much more feasible to carry out $(d, \{pp\})$ measurements with modern electronic equipment and the hope is that, through the use of polarised beams and targets, they will lead to evaluations of the relative phases among the three independent $np \rightarrow pn$ spin–spin amplitudes out to at least $q \approx m_\pi$ [90].

We have been very selective in this review, concentrating our attention on the forward values of the $nd \rightarrow pnn/np \rightarrow pn$ cross section ratio, the (\vec{n}, \vec{p}) polarisation transfer, and the deuteron tensor analysing power in nucleon–deuteron charge-exchange break-up collisions. In the latter cases, we have specialised to the kinematic situations where two of the final nucleons emerge in the 1S_0 state. Under these conditions there are strong connections among the three types of experiment described and we have tried to stress this. However, there is clearly much additional information in the data at larger angles, which we have here generally neglected. We have also avoided discussing the extensive data that have been taken on nuclear targets, where the selectivity of the (\vec{n}, \vec{p}) or $(\vec{d}, \{pp\})$ reactions can be used to identify particular classes of final nuclear states. At the higher energies, these states could even include the excitation of the $\Delta(1232)$ isobar.

Despite the successful measurements, none of the $R_{np}(0)$ data nor those from the exclusive polarised measurements have so far been included in any of the existing phase shift analyses. They have merely been used as a posteriori checks on their predictions. We have argued that they could also provide valuable input into the direct neutron–proton amplitude reconstruction in the backward direction [10]. For any of these purposes it would be highly desirable to control further the range of validity of the models used to interpret the data and, in particular, to examine further the effects of multiple scattering. There remain therefore theoretical as well as experimental challenges to be overcome.

Acknowledgements. We are grateful to J. Ludwig for furnishing us with a partial copy of [31]. Several people gave us further details regarding their own experiments. These include D. Chiladze, M. J. Esten, V. Glagolev, A. Kacharava, S. Kox, M. W. McNaughton, T. Motoyoshi, I. Sick, and C. A. Whitten. There were also helpful discussions with D. V. Bugg, Z. Janout, N. Ladygina, I. I. Strakovsky, E. Stokovsky, and Yu. Uzikov. One of the authors (C.W.) wishes to thank the Institute of Experimental and Applied Physics of the Czech Technical University in Prague, and its director Stanislav Pospíšil, for hospitality and support

during the preparation of this paper. This work has been supported by the research programme MSM 684 077 0029 of the Ministry of Education, Youth, and Sport of the Czech Republic.

REFERENCES

1. Chew G. F. // Phys. Rev. 1950. V. 80. P. 196.
2. Chew G. F. // Phys. Rev. 1951. V. 84. P. 710.
3. Gluckstein R. L., Bethe H. // Phys. Rev. 1950. V. 81. P. 761.
4. Pomeranchuk I. // Dokl. Akad. Nauk SSSR. 1951. V. 77. P. 249.
5. Powell W. M. Report UCRL 1191. Berkeley, 1951.
6. Watson K. M. // Phys. Rev. 1952. V. 88. P. 1163.
7. Shmushkevich I. M. Thesis. Leningrad Phys.-Techn. Inst., 1953.
8. Migdal A. B. // J. Exp. Theor. Phys. (USSR). 1955. V. 28. P. 3; Sov. Phys. JETP. 1955. V. 1. P. 2.
9. Lapidus L. I. // J. Exp. Theor. Phys. (USSR). 1957. V. 32. P. 1437; Sov. Phys. JETP. 1957. V. 5. P. 1170.
10. Lehar F., Wilkin C. // Eur. Phys. J. A. 2008. V. 37. P. 143.
11. Dean N. W. // Phys. Rev. D. 1972. V. 5. P. 1661.
12. Dean N. W. // Ibid. P. 2832.
13. Bugg D. V., Wilkin C. // Nucl. Phys. A. 1987. V. 167. P. 575.
14. Phillips R. J. N. // Rep. Prog. Phys. 1959. V. 22. P. 562; Proc. Phys. Soc. A. 1959. V. 74. P. 652; Nucl. Phys. 1964. V. 53. P. 650.
15. Dass G. V., Queen N. M. // J. Phys. A. 1968. V. 1. P. 259.
16. Clough A. S. et al. // Phys. Rev. C. 1980. V. 21. P. 988.
17. Riley P. J. et al. // Phys. Lett. B. 1981. V. 103. P. 313.
18. Chalmers J. S. et al. // Phys. Lett. B. 1985. V. 153. P. 235.
19. Bugg D. V., Wilkin C. // Ibid. V. 154. P. 243.
20. Bystrický J., Lehar F., Winternitz P. // J. Phys. (Paris). 1978. V. 39. P. 1.
21. Ohlsen G. G. // Rep. Prog. Phys. 1972. V. 35. P. 717.
22. Arndt R. A., Strakovsky I. I., Workman R. L. // Phys. Rev. C. 2000. V. 62. P. 034005; Arndt R. A. et al. // Phys. Rev. C. 2007. V. 76. P. 025209; SAID solutions available from <http://gwdac.phys.gwu.edu>
23. Adams D. et al. // Acta Polytechnica (Prague). 1996. V. 36. P. 11.
24. de Lesquen A. et al. // Eur. Phys. J. C. 1999. V. 11. P. 69.
25. McNaughton M. W. et al. // Phys. Rev. C. 1996. V. 53. P. 1092 and ref. therein.
26. Ahmidouch A. et al. // Eur. Phys. J. C. 1998. V. 2. P. 627 and ref. therein.
27. Bugg D. V. et al. // Phys. Rev. C. 1980. V. 21. P. 1004 and ref. therein.
28. Cladis J. R., Hadley J., Hess W. N. // Phys. Rev. 1952. V. 86. P. 110.
29. Dzhelepov V. P. et al. // Izv. Akad. Nauk. 1955. V. 19. P. 573.
30. Dzhelepov V. P. et al. // Nuovo Cim. Suppl. 1956. V. 3. P. 61.
31. Pagels B. Untersuchung der quasielastischen Ladungsaustauschreaktion $nd \rightarrow pnn$ im Neutronen-energiebereich von 290 bis 570 MeV. Diploma Thesis. Univ. Freiburg im Breisgau, 1988.
32. Larsen R. R. // Nuovo Cim. A. 1960. V. 18. P. 1039.

33. *Dzhelepov V.P.* Recent Investigations on Nucleon–Nucleon Scattering at the Dubna Synchrotron // Proc. of Intern. Conf. on High Energy Phys. / Ed. J. Prentki. CERN. Geneva, 1962. P. 19.
34. *Voitovetskii V.K., Korsunskii I.L., Pazhin Yu.F.* // Nucl. Phys. 1965. V. 69. P. 531.
35. *Wong C. et al.* // Phys. Rev. 1959. V. 116. P. 164.
36. *Measday D.F.* // Phys. Lett. 1966. V. 21. P. 66.
37. *Bonner B.E. et al.* // Phys. Rev. C. 1978. V. 17. P. 664.
38. *Franz J. et al.* // Physica Scripta T. 1999. V. 87. P. 14.
39. *Sharov V.I. et al.* // Eur. Phys. J. C. 2004. V. 37. P. 79.
40. *Lehar F.* // Part. Nucl. 2005. V. 36. P. 501.
41. *Sharov V.I. et al.* // Eur. Phys. J. A. 2009. V. 39. P. 267.
42. *Hofmann J.A., Strauch K.* // Phys. Rev. 1953. V. 90. P. 559.
43. *Batty C.J., Gilmore R.S., Stafford G.H.* // Phys. Lett. 1965. V. 16. P. 137.
44. *Langsford A. et al.* // Nucl. Phys. A. 1967. V. 99. P. 246.
45. *Bjork C.W. et al.* // Phys. Lett. B. 1976. V. 63. P. 31.
46. *Esten M.J. et al.* // Rev. Mod. Phys. 1965. V. 37. P. 533; Nucl. Phys. 1966. V. 86. P. 289.
47. *Glagolev V.V. et al.* // Cent. Eur. J. Phys. 2008. V. 6. P. 781.
48. *Castillejo L., Singh L.S.* // Proc. of Conf. on Nuclear Forces and the Few Body Problem. London, 1960. P. 193.
49. *Aladashvili B.S. et al.* // Nucl. Phys. B. 1975. V. 86. P. 461.
50. *Aladashvili B.S. et al.* // J. Phys. G. 1977. V. 3. P. 7.
51. *Aladashvili B.S. et al.* // Ibid. P. 1225.
52. *Glagolev V.V. et al.* // Eur. Phys. J. A. 2002. V. 15. P. 471.
53. *Shepard P.F. et al.* // Phys. Rev. D. 1974. V. 10. P. 2735.
54. *Bystrický J., Lechanoine-Leluc C., Lehar F.* // J. Phys. (Paris). 1987. V. 48. P. 199.
55. *Bizard G. et al.* // Nucl. Phys. B. 1975. V. 85. P. 14.
56. *Bystrický J., Lehar F.* // Nucleon–Nucleon Scattering Data / Ed. H. Behrens und G. Ebel. Fachinformationszentrum Karlsruhe. 1978 Ed. 1978. Nr. 11-1; 1981 Ed. 1981. Nr. 11-2 and Nr. 11-3.
57. *Bystrický J. et al.* // Landolt–Börnstein. V. 9. Berlin: Springer, 1980.
58. *Binz R.* Untersuchung der spinabhängigen Neutron–Proton Wechselwirkung im Energiebereich von 150 bis 1100 MeV. PhD Thesis. Univ. Freiburg im Breisgau, 1991.
59. *Arndt R.A., Hyslop III J.S., Roper L.D.* // Phys. Rev. D. 1987. V. 35. P. 199.
60. *Glauber R.J., Franco V.* // Phys. Rev. 1967. V. 156. P. 1685.
61. *Reay N.W. et al.* // Phys. Rev. 1966. V. 150. P. 806.
62. *Robertson L.P. et al.* // Nucl. Phys. A. 1969. V. 134. P. 545.
63. *Lisowski P.W. et al.* // Nucl. Phys. A. 1980. V. 334. P. 45.
64. *Jain M., Doolen G.* // Phys. Rev. C. 1973. V. 8. P. 124.
65. *Sakai H. et al.* // Phys. Lett. B. 1986. V. 177. P. 155.
66. *Henneck R. et al.* // Phys. Rev. 1988. V. 37. P. 2224.
67. *Pickar M.A. et al.* // Phys. Rev. C. 1990. V. 42. P. 20.
68. *Zeier M. et al.* // Nucl. Phys. A. 1999. V. 654. P. 541; PhD Thesis. Univ. Basel, 1997.
69. *Henneck R. et al.* // Nucl. Instr. Meth. A. 1987. V. 259. P. 329.
70. *Glöckle W. et al.* // Phys. Rep. 1996. V. 274. P. 107.

71. Anderson B. D. *et al.* // Phys. Rev. C. 1996. V. 54. P. 1531.
72. Sakai H. *et al.* // Phys. Rev. C. 1987. V. 35. P. 344.
73. McNaughton M. W. *et al.* // Phys. Rev. C. 1992. V. 45. P. 2564.
74. Bugg D. V. Private communication noted in [73].
75. Mercer D. J. *et al.* // Phys. Rev. Lett. 1993. V. 71. P. 684.
76. Ellegaard C. *et al.* // Phys. Rev. Lett. 1987. V. 59. P. 974.
77. Ellegaard C. *et al.* // Phys. Lett. B. 1989. V. 231. P. 365.
78. Sams T. PhD Thesis. Niels Bohr Inst. Copenhagen, 1990 (available at www.nbi.dk/sams).
79. Sams T. *et al.* // Phys. Rev. C. 1995. V. 51. P. 1945.
80. Dubois R. *et al.* // Nucl. Phys. A. 1982. V. 377. P. 554.
81. Carbonell J., Barbaro M. B., Wilkin C. // Nucl. Phys. A. 1991. V. 529. P. 653.
82. Kox S. *et al.* // Phys. Lett. B. 1991. V. 266. P. 265.
83. Kox S. *et al.* // Nucl. Phys. A. 1993. V. 556. P. 621.
84. Bäumer C. *et al.* // Phys. Rev. C. 2005. V. 71. P. 044003.
85. Motobayashi T. *et al.* // Nucl. Phys. A. 1988. V. 481. P. 207.
86. Réal J.-S. PhD Thesis. Univ. of Grenoble, 1994.
87. Kox S. Private communication. 2009.
88. Kox S. *et al.* // Nucl. Instr. Meth. A. 1994. V. 346. P. 527.
89. Abbott D. *et al.* // Phys. Rev. Lett. 2000. V. 84. P. 5053.
90. Kacharava A., Rathmann F., Wilkin C. Spin Physics from COSY to FAIR. COSY Proposal. 2005. V. 152; nucl-ex/0511028.
91. Chiladze D. *et al.* // Phys. Lett. B. 2006. V. 637. P. 170.
92. Chiladze D. *et al.* // Eur. Phys. J. A. 2009. V. 40. P. 23.
93. Chiladze D. *et al.* // Phys. Rev. ST Accel. Beams. 2006. V. 9. P. 050101.
94. Schleichert R. *et al.* // IEEE Trans. Nucl. Sci. 2003. V. 50. P. 301.
95. Peterson T. *et al.* // Nucl. Instr. Meth. A. 2004. V. 527. P. 432.

Received on October 23, 2009.